

Mean First Passage Time of the Symmetric Noisy Voter Model with Arbitrary Initial and Boundary Conditions

Rytis Kazakevičius, Aleksejus Kononovicius

Institute of Theoretical Physics and Astronomy, Vilnius University

Abstract

Models of imitation and herding behavior often underestimate the role of individualistic actions and assume symmetric boundary conditions. However, real-world systems (e.g., electoral processes) frequently involve asymmetric boundaries. In this study, we explore how arbitrarily placed boundary conditions influence the mean first passage time in the symmetric noisy voter model, and how individualistic behavior amplifies this asymmetry. We derive exact analytical expressions for mean first passage time that accommodate any initial condition and two types of boundary configurations: (i) both boundaries absorbing, and (ii) one absorbing and one reflective. In both scenarios, mean first passage time exhibits a clear asymmetry with respect to the initial condition, shaped by the boundary placement and the rate of independent transitions. Symmetry in mean first passage time emerges only when absorbing boundaries are equidistant from the midpoint. Additionally, we show that Kramers' law holds in both configurations when the rate of independent transitions is large. Our analytical results are in excellent agreement with numerical simulations, reinforcing the robustness of our findings.

1 Introduction

The mean first passage time (abbr. MFPT) is a tool widely used in various fields such as quantum statistical mechanics [1–7], laser physics [8, 9], chemistry [10–12], biology [13–15]. It is particularly prominent in the research on stochastic processes and random walks [16, 17], and most recently in the context of target search problems [18]. The MFPT, also known as the first hitting time or first detection time, refers to the average time it takes for a system initially in one specific state (or states) to reach a different specific state (or states) for the first time. The MFPT can be directly calculated from the first passage time distribution (abbr. FPTD) [18–20]; however, for many stochastic processes, the FPTD is known only in the form of an infinite series [21]. In certain cases, e.g., for birth–death processes [22], MFPT can be used to obtain a reasonable approximation for the FPTD. In sociophysics, which applies physics-based methods to social phenomena, MFPT is increasingly used to study aspects of human behavior, such as polarization and segregation in voting dynamics [23], and how the trading strategies affect the financial markets [24]. Voter models, in particular, are employed to simulate social networks and the influence of mass media on opinion formation [25], statistical voting patterns [26–29], polarization, and consensus formation [30, 31]. Comparing voter model predictions against empirical social network data analysis is also a promising research direction [32–36]. While there are many other opinion dynamics models [37–39], only voter models have been as well-suited for the MFPT analysis [40]. In this context, the investigation of MFPT within the framework of voter models constitutes a compelling direction for future research, with the theoretical and applied potential.

An extensive body of work exists that either analytically derives, or explores numerically, the MFPT for a range of modified and extended versions of the voter model [31, 40–43]. Most of these works focus on evaluating the consensus time, which refers to the average time for a polarized system to reach a consensus state for the first time [40–43]. It has also been applied to quantify other characteristic times, such as the opinion switching

time [44] and opinion polarization time [31]. Therefore, the analysis of MFPT in voter models helps researchers understand how fast a population can change, how this the pace of change depends on system characteristics [31] and variety of opinion formation mechanisms [40]. By providing a quantitative framework for the expected timing of transitions between the states, MFPT enables the exploration of communication patterns, influence, and collective decision-making in networks [25, 32, 45]. This exploration could have potential applications for financial risk management [24], as the noisy voter model (often under the name of Kirman model [46]) has been shown to be a good model for opinion dynamics in the financial markets as well [47–49].

Despite the growing interest in first passage time statistics for various modifications of the voter models, most studies have mainly relied on numerical simulations [41–43, 50]. Furthermore, many of the earlier works have set out to explore how the MFPT scales with the system size [40, 42, 51] but have neglected scaling based on other parameters, such as independent transition rates, introduced in other common modifications of the voter model. Notably [31, 44] have recently explored MFPT dependence on the independent transition rates. Even in these works analytical approximations for MFPT have been obtained only in limited cases, such as for low independent transition rates [44] or for fixed boundary conditions [31]. Therefore, a general framework that analyzes MFPT dependence on transition rates and boundary conditions can still be developed further.

To simplify the analytical derivation, the MFPT dependence on the initial condition can be made symmetric by choosing symmetric boundary conditions [52]. Yet this assumption is highly restrictive, as real-life problems may have inherent asymmetry. For example, in many multi-party proportional representation systems, a political party must surpass a minimum vote threshold, often 4% or 5%, to gain representation in the parliament [53]. On the other hand, a party would be considered successful (and likely to win a multi-party election) if it received more than 30% of the votes. Thus, a natural asymmetry in the political expectations arises. Consequently, in this work, we focus on asymmetry in the MFPT, as it better captures the non-uniform nature of threshold-based systems and decision-making processes in social systems. The primary aim of this study is to explore how asymmetry in boundary conditions influence asymmetry observed in MFPT and how asymmetric MFPT scales as independent transition rates grow larger. To facilitate the present analysis, we instead assume symmetry in the independent transition rates, an assumption we anticipate relaxing in the future.

This paper is organized as follows. In Section 2, we describe our definition and approach to the numerical simulation of the noisy voter model. In Section 3, we present the main analytical results and compare them against the numerical simulations. In Section 4, we discuss we obtained results with a focus on their validation and possible applications. Conclusions and future outlook follow in Section 5. In the main body of the text, to keep it more approachable and concise, we have skipped some of the derivation steps, these are discussed in detail in the A (derivation of the ordinary differential equation for MFPT), B (solution of the ordinary differential equation for MFPT) and C (analysis of a few selected special cases).

2 Noisy voter model

The original formulation of the voter model [54] involved spatial competition between two species. In the original model, during every simulation step, a random site on rectangular grid was selected, and then its contents (a single individual) were replaced by a copy of an individual from a neighboring site. This copying mechanism was well received by the opinion dynamics community [37, 55], as with a slight change in terminology, it can be seen to be equivalent to conformist behavior in social response theory [56, 57]. Here, we will consider a generalization of the voter model, which incorporates not only peer copying behavior but also spontaneous transitions without interaction with a peer. Because spontaneous transitions are similar to noise, this generalization is often referred to as the noisy voter model. This generalization of the voter model was originally introduced in [58], but a remarkably similar model was independently proposed in [46] with economic modeling in mind. Thus, some works refer to this model as Kirman’s model or the herding model [47, 48, 59], though the microscopic foundation of both models is mostly the same. The noisy voter model is one of the most prevalent models in sociophysics [37]. It exhibits rich phenomenology and has successfully been used to replicate electoral data

across different countries [26–29].

Let us formulate the noisy voter model as follows. Let there be a fixed number N of particles (also agents or voters) in the simulated system. Any particle can occupy any of the two available states. Let us label the states as “0” and “1”. Transitions between the states occur either independently (at rate r_i , where the index i would match the destination state label) or due to the interaction with other particles in the destination state (let the interaction rate between any two particles be h). If X denotes the number of particles in state “1”, then a single transition will change the X by at most one step (up or down). Under these assumptions and with the selected notation, the transition rates with respect to X are given by:

$$\lambda(X \rightarrow X + 1) = \lambda^+ = (N - X)(r_1 + hX), \quad \lambda(X \rightarrow X - 1) = \lambda^- = X(r_0 + h[N - X]). \quad (1)$$

Because the transition rates encode a one-step process, we employ the birth–death process formalism [60] to derive a stochastic differential equation (abbr. SDE) that approximates the discrete noisy voter model:

$$dx = \frac{\lambda^+ - \lambda^-}{N} dt + \sqrt{\frac{\lambda^+ + \lambda^-}{N^2}} dW \approx h[\varepsilon_1(1 - x) - \varepsilon_0 x] dt + \sqrt{2hx(1 - x) + \frac{h\varepsilon_1}{N}(1 - x) + \frac{h\varepsilon_0}{N}x} dW. \quad (2)$$

Here, N denotes the number of agents. The equation above is suitable for analyzing finite-size effects and related phenomena. However, in this study, we focus on the large- N regime. Taking the limit $N \rightarrow \infty$ and assuming that the transition rates are much smaller than N , the SDE governing the fraction of agents in state “1”, i.e., $x = \frac{X}{N}$, simplifies to

$$dx = h[\varepsilon_1(1 - x) - \varepsilon_0 x] dt + \sqrt{2hx(1 - x)} dW. \quad (3)$$

We interpret the SDE above in the Itô sense, where W denotes the standard Wiener process. In this formulation, we introduce a dimensionless notation for the independent transition rates, $\varepsilon_i = \frac{r_i}{h}$. This choice decouples the overall timescale of the process (controlled by h) from the shape of its dynamics (determined by ε_i). Thus, without loss of generality, let us set $h = 1$ and consider only the impact of independent transition rates ε_i . For $h \neq 1$, the obtained mean first-passage times would need to be trivially multiplied by h .

Obtaining the steady-state distribution of the process described by Eq. (3) is trivial [20]. It can easily be shown to be the Beta distribution with respective shape parameters equal to ε_i . The probability density function of the steady-state distribution is given by:

$$P_\infty(x) = \frac{\Gamma(\varepsilon_0 + \varepsilon_1)}{\Gamma(\varepsilon_0)\Gamma(\varepsilon_1)} x^{\varepsilon_1 - 1} (1 - x)^{\varepsilon_0 - 1}. \quad (4)$$

Notably, steady-state distribution can also be derived for the discrete noisy voter model with finite N . It follows a Beta-binomial distribution with the number of trials equal to N and the shape parameters given by ε_i (see Appendix B in [61]). The independent transition rates, ε_0 and ε_1 , literally control the shape of the Beta distribution. If both are less than 1, $P_\infty(x)$ is bimodal (i.e., the distribution has a U-shape). If both are greater than 1, $P_\infty(x)$ is unimodal (i.e., the distribution has a bell-shape). If $\varepsilon_0 = \varepsilon_1 = 1$, then the Beta distribution reduces to the uniform distribution. If the values of the independent transition rates differ, $P_\infty(x)$ will become skewed to the right (if $\varepsilon_1 > \varepsilon_0$) or to the left (if $\varepsilon_1 < \varepsilon_0$). In this work, we focus on a symmetric noisy voter model, i.e., $\varepsilon_0 = \varepsilon_1 = \varepsilon$.

We numerically solve Eq. (3), with $h = 1$ and $\varepsilon_0 = \varepsilon_1 = \varepsilon$, using Euler–Maruyama method [62]. Starting from the initial condition x_0 , we iterate the following difference equation (in it Δt is the constant time step, and ξ_i are standard normal random variables),

$$x_{i+1} = x_i + \varepsilon(1 - 2x_i) \Delta t + \sqrt{2x_i(1 - x_i)} \Delta t \xi_i, \quad (5)$$

until either lower boundary L or higher boundary H is passed (we require that $L \leq x_0 \leq H$). If that boundary

is absorbing, we record the time, $T = (i + 1) \Delta t$, as a new sample of the first passage time and restart the simulation. If the boundary condition is reflective, then the new x_{i+1} value is clipped to the range of valid values (e.g., if after iterating the difference equation we would have $x_{i+1} \leq L$, we instead set $x_{i+1} = L$). To constrain the simulation, we require that any first passage time would be at most T_{\max} . If $(i + 1) \Delta t > T_{\max}$ without reaching an absorbing boundary condition, we ignore the current run and restart the simulation. Unless noted otherwise, the numerical results reported here have been obtained with $\Delta t = 10^{-5}$, $T_{\max} = 10^6$ and by taking 10^5 samples. Alternatively, a variable time step method [63] or higher-order methods [62] (e.g., the Milstein approximation method) could be used; however, these methods would require more computational resources without producing a qualitative impact on the obtained results.

The code implementing the described approach to sampling the MFPT from the symmetric noisy voter model, along with the relevant scripts reproducing all the figures presented in the later sections, is available on GitHub [64].

3 The mean first passage time

3.1 General solution

If first-passage time distribution (abbr. FPTD), $p_T(T)$, of the stochastic process has a closed-form expression, mean first-passage time (abbr. MFPT) can be calculated directly

$$\bar{T} = \int_0^\infty T p_T(T) dT. \quad (6)$$

However, for many stochastic processes, the FPTD can be expressed analytically only as an infinite sum, rather than as a closed-form expression [21]. Even when the FPTD can be expressed in terms of elementary or special functions, the integral above often remains analytically intractable and must be evaluated numerically [19]. Therefore, a more commonly employed approach in physics to obtain the MFPT is to use the time-backward Fokker–Planck equation.

For the symmetric noisy voter model described by Eq. (3), with $h = 1$ and $\varepsilon_0 = \varepsilon_1 = \varepsilon$, the corresponding Fokker–Planck is

$$\frac{\partial}{\partial t} P(x, t | x_0, 0) = -\varepsilon \frac{\partial}{\partial x} [(1 - 2x) P(x, t | x_0, 0)] + \frac{\partial^2}{\partial x^2} [x(1 - x) P(x, t | x_0, 0)]. \quad (7)$$

It can be shown that the time-backward Fokker–Planck equation [20] associated with the Fokker–Planck equation above is

$$\frac{\partial}{\partial t} P(x, t | x_0, 0) = \varepsilon(1 - 2x_0) \frac{\partial}{\partial x_0} P(x, t | x_0, 0) + x_0(1 - x_0) \frac{\partial^2}{\partial x_0^2} P(x, t | x_0, 0). \quad (8)$$

In the A, Eqs. (40)–(45), we have shown that the time-backward Fokker–Planck equation above leads to the following ordinary differential equation (abbr. ODE) for the MFPT:

$$x_0(1 - x_0) \frac{d^2}{dx_0^2} \bar{T} + \varepsilon(1 - 2x_0) \frac{d}{dx_0} \bar{T} = -1. \quad (9)$$

To derive the ODE above from the Fokker–Planck equation, we assumed that the parameter ε is time-independent. This is a common assumption in the literature [37, 39, 58]. Although, some recent works have shown that for certain problems it is convenient to treat ε as being time-dependent [65]. Consequently, ODE (9) is not applicable to scenarios involving time-dependent transition rates. For a general framework to derive ODEs for the MFPT see Refs. [19, 20]. The obtained equation for the MFPT is a second-order ODE and must be supplemented by two boundary conditions. Therefore, the MFPT problem is well-posed only as an escape from a bounded domain problem [52]. This approach cannot be applied to problems with only one absorbing boundary condition. In such cases, alternative approaches can be taken, such as perturbation techniques [66–69], Laplace

transforms [70], or a direct solution of backward Fokker–Planck equation [17]. In this paper, we obtain a general solution of the Eq. (9) (see B for more details), which specifies the MFPT for the symmetric noisy voter model.

Let the symmetric noisy voter model process start at x_0 . Let the boundary conditions be placed at L and H , so that $0 \leq L \leq x_0 \leq H \leq 1$. These boundary conditions confine the process to a clipped interval $[L, H]$ instead of the natural interval $[0, 1]$. Then in case of two absorbing boundary conditions, we obtain the MFPT (see B for derivation)

$$\bar{T}_{LH} = \frac{\bar{T}_p(H) \beta_{1-L} - \bar{T}_p(L) \beta_{1-H}}{\beta_{1-H} - \beta_{1-L}} + \frac{\bar{T}_p(L) - \bar{T}_p(H)}{\beta_{1-H} - \beta_{1-L}} \beta_{1-x_0} + \bar{T}_p(x_0). \quad (10)$$

In the above $\beta_z = \beta_z(1 - \varepsilon, 1 - \varepsilon)$ is the incomplete beta function (the frequently repeated arguments have been omitted for brevity), and $\bar{T}_p(z)$ is a particular solution of Eq. (9), which is given by

$$\bar{T}_p(z) = \frac{1}{\Gamma(2\varepsilon) \Gamma(1 - \varepsilon)} G_{3,3}^{2,3} \left(z \left| \begin{matrix} 1, 1, 2(1 - \varepsilon) \\ 1, 1 - \varepsilon, 0 \end{matrix} \right. \right). \quad (11)$$

Here $\Gamma(\varepsilon)$ is the gamma function, and $G_{p,q}^{m,n} \left(z \left| \begin{matrix} a_1, a_2, \dots, a_p \\ b_1, b_2, \dots, b_q \end{matrix} \right. \right)$ is Meijer G -function.

If the boundary condition at L is reflective instead (this choice, in the context of the voter model, could be interpreted as representing an inflexible voter base [71–74]), while the boundary condition at H remains absorbing, the MFPT is given by (see B for derivation)

$$\bar{T}_r = \left[\frac{\Gamma(\varepsilon) \Gamma(\varepsilon)}{\Gamma(2\varepsilon)} - \beta_L(\varepsilon, \varepsilon) \right] [\beta_{1-x_0}(1 - \varepsilon, 1 - \varepsilon) - \beta_{1-H}(1 - \varepsilon, 1 - \varepsilon)] + \bar{T}_p(x_0) - \bar{T}_p(H). \quad (12)$$

If boundary condition at H would be reflective (this choice, in the context of the voter model, could be interpreted as representing an inflexible opposition [71–74]), and boundary condition at L would be absorbing, the above solution would still apply with just swapping of the L and H symbols.

3.2 Obtaining reduced mean first passage time expressions for certain ε

Eqs. (10) and (12) constitute the main analytical results of this paper. At first glance, these MFPT expressions may appear problematic to evaluate due to the presence of special functions. However, for certain values of the independent transition rate, these special functions may be reduced to expressions involving basic functions. In particular, significant simplification occurs when $\varepsilon = \frac{n}{2}$ with $n \in \mathbb{N}$, due to the mathematical properties of the special functions involved. Notably, special attention should be given to the cases with integer ε , as in these cases the standard relation between the incomplete beta function and the hyper-geometric function breaks down. For the integer ε , $\beta_{1-z}(1 - \varepsilon, 1 - \varepsilon)$, $\beta_z(\varepsilon, \varepsilon)$ and $\bar{T}_p(z)$ must be evaluated directly from Eqs. (83) and (86). Thus, let us consider the first few values, i.e., $\varepsilon = 0, \frac{1}{2}, 1, \frac{3}{2}, 2$ and $\frac{5}{2}$.

For the considered ε values, one of the parametrizations of the incomplete beta function can be reduced to

$$\beta_{1-z}(1 - \varepsilon, 1 - \varepsilon) = \begin{cases} 1 - z, & \text{for } \varepsilon = 0, \\ 2 \arcsin(\sqrt{1 - z}), & \text{for } \varepsilon = \frac{1}{2}, \\ \ln(1 - z) & \text{for } \varepsilon = 1, \\ \frac{2(1-2z)}{\sqrt{z(1-z)}}, & \text{for } \varepsilon = \frac{3}{2}, \\ \frac{1-2z}{z(1-z)} + 2(\ln(z) - \ln(1 - z)), & \text{for } \varepsilon = 2, \\ \frac{2(16z^3 - 24z^2 + 6z + 1)}{3z^{3/2}(1-z)^{3/2}}, & \text{for } \varepsilon = \frac{5}{2}. \end{cases} \quad (13)$$

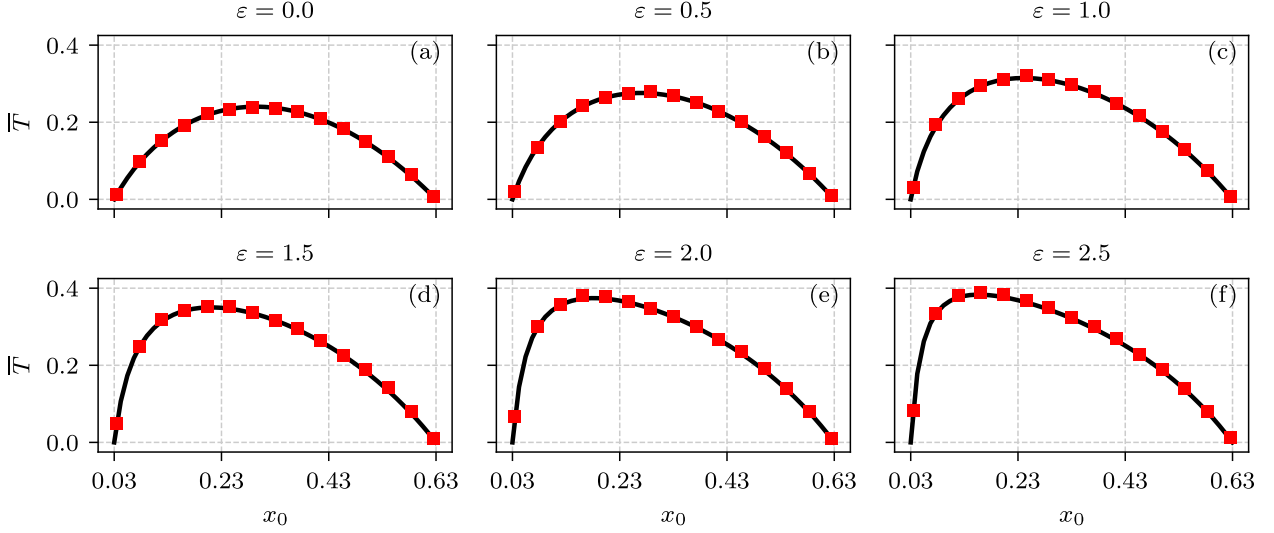


Figure 1: The mean first passage time \bar{T} dependence on the initial condition x_0 with various values of independent transition rate ε for the case with absorbing boundary conditions at L and H . The black curves correspond to Eq. (10), while the red squares represent estimates obtained by numerical simulation of Eq. (3) with $h = 1$ and $\varepsilon_0 = \varepsilon_1 = \varepsilon$. Boundary conditions were placed at $L = 0.03$ and $H = 0.63$.

Similarly, the other parametrization can be reduced to

$$\beta_z(\varepsilon, \varepsilon) = \begin{cases} \ln(z), & \text{for } \varepsilon = 0, \\ 2 \arcsin(\sqrt{z}), & \text{for } \varepsilon = \frac{1}{2}, \\ z, & \text{for } \varepsilon = 1, \\ \frac{1}{4} \left((2z-1) \sqrt{z(1-z)} + \arcsin(\sqrt{z}) \right), & \text{for } \varepsilon = \frac{3}{2}, \\ \frac{1}{6} (3-2z) z^2, & \text{for } \varepsilon = 2, \\ \frac{1}{64} \left((16z^3 - 24z^2 + 2z + 3) \sqrt{z(1-z)} + 3 \arcsin(\sqrt{z}) \right), & \text{for } \varepsilon = \frac{5}{2}. \end{cases} \quad (14)$$

Likewise, the particular solution can be reduced to

$$\bar{T}_p(z) = \begin{cases} (z-1) \ln(1-z) - z \ln(z), & \text{for } \varepsilon = 0, \\ \frac{1}{2} \left(\pi^2 + (2 \operatorname{arccosh}(\sqrt{z}))^2 \right), & \text{for } \varepsilon = \frac{1}{2}, \\ \ln(z) - \ln(1-z), & \text{for } \varepsilon = 1, \\ \frac{1}{2} \left(\frac{(2z-1) \operatorname{arccos}(\sqrt{z})}{\sqrt{z(1-z)}} - 1 \right), & \text{for } \varepsilon = \frac{3}{2}, \\ \frac{1}{6} \left(\frac{z}{z-1} + 2 \ln(1-z) \right), & \text{for } \varepsilon = 2, \\ \frac{(20z^2 - 20z - 3) \sqrt{z(1-z)} - 3(16z^3 - 24z^2 + 6z + 1) \operatorname{arccos}(\sqrt{z})}{96z^{3/2}(1-z)^{3/2}}, & \text{for } \varepsilon = \frac{5}{2}. \end{cases} \quad (15)$$

Relevant derivations for a few of these special cases are provided in C. The reduced expressions enable a more transparent analytical treatment of the MFPT dependence on the initial condition. These expressions also facilitate a comparison between analytical expressions and results of the numerical simulation (see Figs. 1 and 2).

Figures 1 and 2 show an excellent agreement between the obtained MFPT expressions and numerical simulation results for the two distinct boundary problems. For the both considered boundary problems, the dependence of MFPT on the independent transition rate is highly asymmetric. For the case with two absorbing boundaries (see Fig. 1), the degree of asymmetry increases with ε as the MFPT peak shifts away from the middle of the allowed x value range towards the boundary condition which lies closer to the natural boundary. Also, the

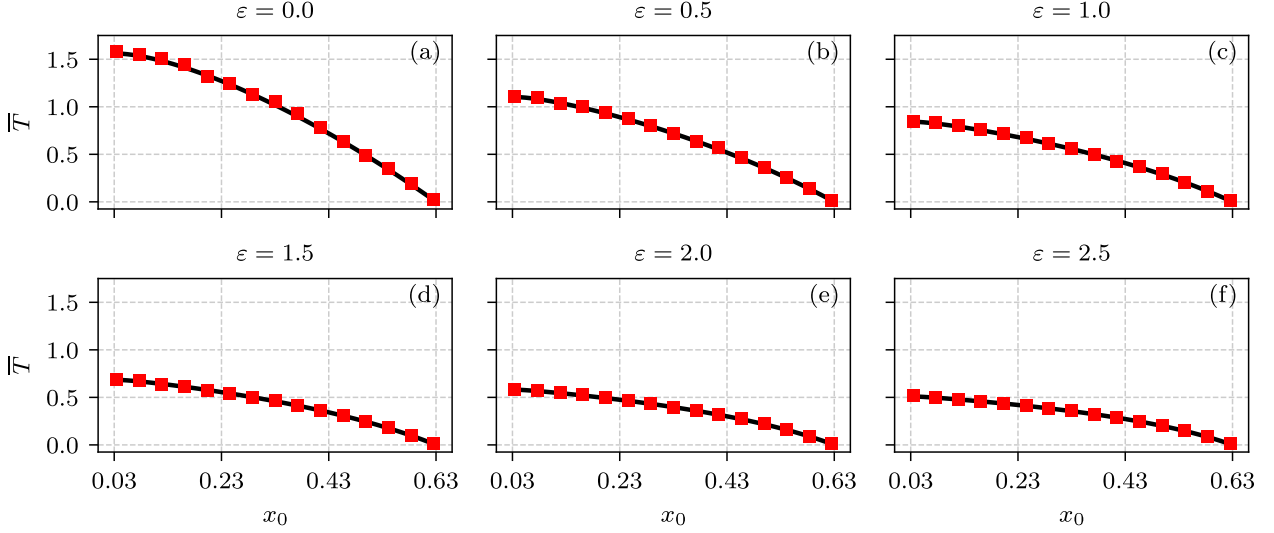


Figure 2: The mean first passage time \bar{T} dependence on the initial condition x_0 with various values of independent transition rate ε for the case with reflective boundary condition at L and absorbing boundary condition at H . The black curves correspond to Eq. (12), while the red squares represent estimates obtained by numerical simulation of Eq. (3) with $h = 1$ and $\varepsilon_0 = \varepsilon_1 = \varepsilon$. In all instances boundary conditions were placed at $L = 0.03$ and $H = 0.63$.

maximum MFPT grows larger with ε . For the case with one reflective and one absorbing boundary (see Fig. 2), the maximum MFPT always lies at the reflective boundary, but the maximum \bar{T} decreases with ε . Though, as will be shown in Section 3.5, the dependence of \bar{T} on ε in both considered cases is not as trivial as can be observed from Figs. 1 and 2.

3.3 Detailed analysis of the $\varepsilon = 0$ case

Here, let us consider $\varepsilon = 0$ case in more detail. This case yields the most compact and tractable expressions for the MFPT within our framework. This case also proves particularly interesting as it coincides with the original voter model on a complete graph (i.e., if any particle may interact with any other particle).

Let us insert appropriate replacements for the incomplete beta function, taken from Eqs. (13) and (14), and the particular solution, Eq. (15), into Eq. (10). Then Eq. (10) simplifies to

$$\bar{T}_{LH}(x_0|\varepsilon=0) = \frac{Lf(H) - Hf(L)}{H-L} + \frac{f(L) - f(H)}{H-L}x_0 + f(x_0). \quad (16)$$

Here we have introduced a placeholder function

$$f(z) = (z-1)\ln(1-z) - z\ln(z), \quad (17)$$

which allows us to greatly simplify the MFPT expression above. Notably, it can be shown that MFPT dependence on the initial condition reaches maximum value at

$$x_{0,\max} = \max [\bar{T}_{LH}(x_0|\varepsilon=0)] = \frac{1}{2} \left(1 - \tanh \left[\frac{f(H) - f(L)}{2(H-L)} \right] \right). \quad (18)$$

The meaning of the placeholder function might not be immediately obvious, but if we let the absorbing boundaries coincide with the natural boundaries, i.e., $L = 0$ and $H = 1$, MFPT becomes

$$\bar{T}_{01}(x_0|\varepsilon=0) = (x_0-1)\ln(1-x_0) - x_0\ln(x_0) = f(x_0). \quad (19)$$

In the literature, MFPT to the natural boundaries of the voter model is commonly referred to as the mean consensus time [52]. It represents the average time required for all particles to end up in the same state (either “0” or “1”), thereby achieving consensus. Notably, the expression for the mean consensus time is identical to $f(x_0)$; hence, the placeholder function above represents this quantity. The analytical expression for the mean consensus time has been derived in numerous previous studies and is well known to involve logarithmic terms across various extensions of the voter model [52, 75–78]. Although, to the best of our knowledge, the generalized MFPT expression, Eq. (16), has not yet been studied in detail. Therefore, we continue with the analysis of the generalized MFPT expression, which reveals how the symmetry or asymmetry of the MFPT can be controlled through the choice of boundary conditions.

The meaning of the first term in Eq. (16) becomes obvious by inserting $x_0 = L$ or $x_0 = H$ into the equation. Namely, the first term ensures that MFPT will be zero at the boundary conditions L and H .

The meaning of the second term in Eq. (16) is revealed by choosing symmetric boundary conditions, i.e., $L = \frac{1}{2} - d$ and $H = \frac{1}{2} + d$ (with $0 < d \leq \frac{1}{2}$). With these boundary conditions, the second term disappears, which allows us to conclude that this term is responsible for the asymmetry in the MFPT. The term disappears because the placeholder (consensus time) function is symmetric in respect to the midpoint, i.e., $f(\frac{1}{2} - z) = f(\frac{1}{2} + z)$ (with $0 \leq z \leq \frac{1}{2}$) or, alternatively, $f(z) = f(1 - z)$ (with $0 \leq z \leq 1$). Thus, if the boundary conditions are placed symmetrically to the midpoint, MFPT will also be symmetric in respect to the midpoint,

$$\bar{T}_{LH}(x_0|\varepsilon=0) = \bar{T}_{LH}(1-x_0|\varepsilon=0), \quad \text{if } L = \frac{1}{2} - d \text{ and } H = \frac{1}{2} + d. \quad (20)$$

The asymmetry in the MFPT arises from the nonlinear, position-dependent diffusion coefficient in the Fokker–Planck equation, Eq. (7). Specifically, the diffusion term $x(1-x)$ increases from zero at $x=0$, reaches its maximum at $x=\frac{1}{2}$, and then goes back to zero at $x=1$. This means that the rate of diffusion is not uniform across the interval. If one boundary is placed near a region of slower diffusion (close to 0 or 1) and the other near a region of greater diffusion (closer to $\frac{1}{2}$), the particle is more likely to reach the latter boundary first. For instance, if L is close to 0 and $H = \frac{1}{2}$, and the initial condition x_0 lies between them, the particle tends to reach H faster because the diffusion coefficient is significantly larger close to H than near L . This contrasts with the standard Wiener process, where the diffusion coefficient is constant. In that case, when the process is bounded in the interval $[L, H]$, the MFPT is symmetric with respect to the midpoint $\frac{H+L}{2}$, regardless of the absolute placement of the boundaries.

However, in real-life applications, especially for social processes, symmetric boundary problems are quite rare. For example, in many proportional representation systems, a political party must surpass a minimum vote threshold, often 4% or 5%, to gain representation in parliament [53]. Though, to win an election a party does not need to gain 95% or 96% of the votes, as usually top parties in democratic multi-party elections gain roughly 30% to 40% of votes. Thus, some important real-life problems involves asymmetric boundaries. Moreover, sociopolitical dynamics, such as incumbency advantage [79], media influence and strategic voting [80], further skew the outcome distribution. Thus, we analyze a more general asymmetric problem instead.

For the reflective lower boundary, given $L > 0$, we have

$$\bar{T}_r(x_0|\varepsilon=0) = (H-x_0)g(L) - f(H) + f(x_0), \quad (21)$$

where $g(z)$ is a placeholder function given by

$$g(z) = \ln(1-z) - \ln(z) = 2 \arctan(1-2z). \quad (22)$$

It effectively encodes the attraction towards the reflective boundary (i.e., it accounts for the time wasted moving towards the reflective boundary). Due to this attraction, the maximum MFPT, for the case with reflective boundary at L , is located at the reflective boundary L .

Note that the discussion surrounding the case with reflective boundary at L above applies only when $L > 0$.

Similarly, if the reflective boundary condition would be placed at H instead, then the discussion would apply only for $H < 1$. This is because a reflective boundary at $L = 0$ (or $H = 1$) would not work as intended. Given that $\varepsilon = 0$, it is obvious that the drift term disappears from the Fokker–Planck equation, Eq. (7), while the diffusion term goes to zero at the natural boundaries, $x = 0$ and $x = 1$. Consequently, at the natural boundaries there would be no force (deterministic or stochastic) to push the process away from it, and the process would get stuck (or, in other words, absorbed) at the natural boundary instead of the being reflected.

3.4 Analysis of the $\varepsilon = \frac{1}{2}$ case

This case also yields compact and tractable MFPT expressions within our approach. Let us insert appropriate replacements for the incomplete beta function, taken from Eqs. (13) and (14), and the particular solution, Eq. (15), into Eq. (10). Then for two absorbing boundaries, we have that

$$\bar{T}_{LH} \left(x_0 | \varepsilon = \frac{1}{2} \right) = \frac{1}{2} [\arcsin(2H - 1) - \arcsin(2x_0 - 1)] \cdot [\arcsin(2x_0 - 1) - \arcsin(2L - 1)]. \quad (23)$$

It can be shown that the MFPT maximum, in the case with two absorbing boundaries, is located at

$$x_{0,\max} = \max \left[\bar{T}_{LH} \left(x_0 | \varepsilon = \frac{1}{2} \right) \right] = \frac{1}{2} \left[1 + \sin \left(\frac{\arcsin(2H - 1) + \arcsin(2L - 1)}{2} \right) \right]. \quad (24)$$

From the above it is trivial to see that with symmetric absorbing boundaries, $L = \frac{1}{2} - d$ and $H = \frac{1}{2} + d$ (with $0 < d \leq \frac{1}{2}$), the MFPT maximum would be located at the midpoint.

By inserting the appropriate replacements from Eqs. (13) – (15) into Eq. (12), we obtain the MFPT dependence with reflective lower boundary, $L > 0$,

$$\begin{aligned} \bar{T}_r \left(x_0 | \varepsilon = \frac{1}{2} \right) &= \frac{1}{2} [\arcsin(2H - 1) - \arcsin(2x_0 - 1)] \\ &\cdot [\arcsin(2H - 1) - 2\arcsin(2L - 1) + \arcsin(2x_0 - 1)]. \end{aligned} \quad (25)$$

Once again the MFPT maximum when one reflective boundary would be located at the reflective boundary.

Using similar reasoning as in the previous subsection, one can show that

$$\bar{T}_{LH} \left(x_0 | \varepsilon = \frac{1}{2} \right) = \bar{T}_{LH} \left(1 - x_0 | \varepsilon = \frac{1}{2} \right), \quad \text{if } L = \frac{1}{2} - d \text{ and } H = \frac{1}{2} + d. \quad (26)$$

The condition necessary to obtain MFPT symmetry is the same as in the $\varepsilon = 0$ case. As shown in C, when $\varepsilon = 1$ or $\varepsilon = \frac{3}{2}$, choosing symmetric boundaries also yields symmetric MFPT. In principle, the same approach can be applied to any $\varepsilon = \frac{n}{2}$, with $n \in \mathbb{N}$, since the MFPT expressions involve trigonometric, logarithmic, and polynomial functions, all of which exhibit inherent symmetries. We therefore speculate that this symmetry might hold for arbitrary values of ε . While we haven't been able to prove this analytically, analysis by numerical simulation supports our intuition (see Fig. 3 (a)).

Conducting the same numerical analysis with asymmetric boundary conditions (see Fig. 3 (b)) seems to indicate that $x_{0,\max}$ tends towards boundary condition, which is closest to the natural boundary condition. In Fig. 3 (b), the lower boundary condition is closer to the natural boundary condition (0.1 is closer to 0, than 0.7 to 1), thus we observe that the MFPT maximum shifts to the lower values as ε increases. This behavior can be examined in more detail by fixing L and exploring how $x_{0,\max}$ depends on the location of the higher boundary condition, H . Results of the additional numerical analysis, shown in Fig. 4, quantitatively confirm the qualitative intuition obtained from inspecting Fig. 3 (b). In other words, $x_{0,\max}$ indeed tends towards the boundary condition closer to the natural boundary condition (all colored curves are below the dashed midpoint line for $H < 0.95$, and are above the dashed midpoint line for $H > 0.95$), while the deviation from the midpoint grows larger as ε increases.

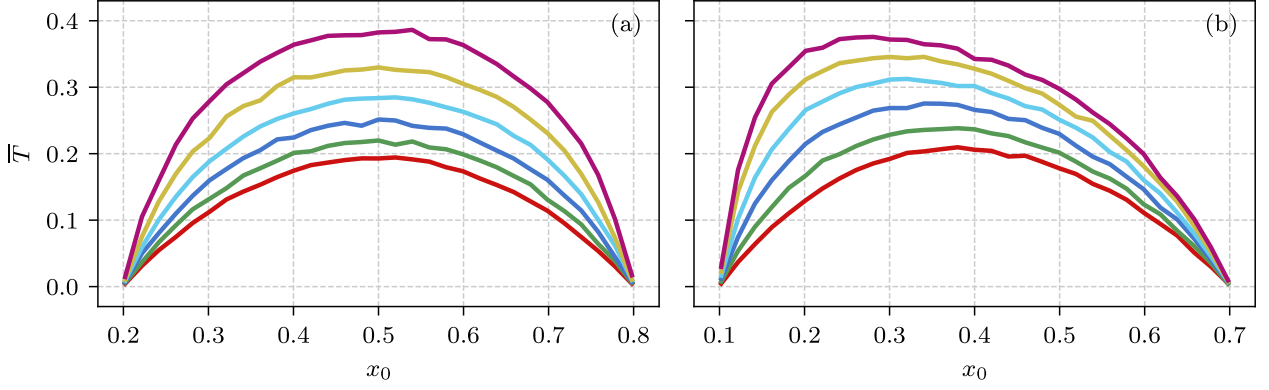


Figure 3: The mean first passage time dependence \bar{T} on the initial condition x_0 with symmetric absorbing boundaries (a), and with asymmetric absorbing boundaries (b). Colored curves show the MFPT dependence obtained by numerical simulation with different rates: $\varepsilon = 0$ (red curves), 0.8 (green), 1.6 (blue), 2.4 (cyan), 3.2 (yellow), 4.0 (magenta). Boundary conditions for the symmetric case (subfigure (a)) were placed at $L = 0.2$ and $H = 0.8$, for the asymmetric case (subfigure (b)) they were placed at $L = 0.1$ and $H = 0.7$.

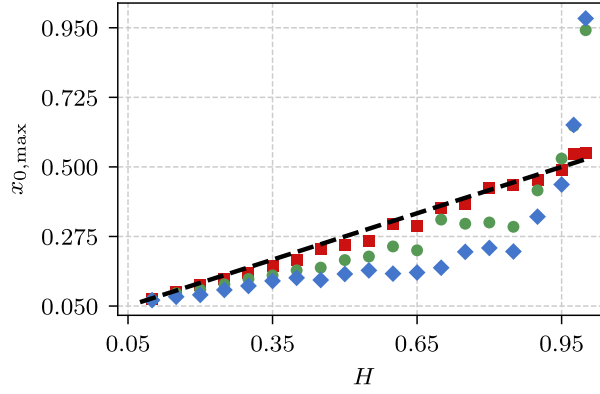


Figure 4: Numerically simulated dependence of $x_{0,\max}$ on the placement of the asymmetric absorbing boundary conditions. Lower boundary is fixed at $L = 0.05$, while the higher boundary H is treated as an independent variable. Dashed black line highlights the midpoint between the boundary conditions, $\frac{H+L}{2}$. Colored symbols show numerical simulation results obtained with different rates: $\varepsilon = 0$ (red squares), 1.6 (green circles), 3.2 (blue diamonds).

3.5 Mean first passage time scaling dependence on ε

MFPT scaling behavior can also be reduced to a simpler expression by considering the dependence on ε in the large ε limit. In A, Eqs. (73) – (79), we have shown that Eq. (12) can be approximated by

$$\bar{T}(\varepsilon) \simeq \frac{2\sqrt{\pi}}{2^{2\varepsilon}\varepsilon^{3/2}} \cdot \frac{H}{(1-H)^\varepsilon H^\varepsilon} = \frac{2\sqrt{\pi}H}{\varepsilon^{3/2}} e^{\varepsilon \ln[\frac{1}{4H(1-H)}}. \quad (27)$$

In A, we demonstrate that Eq. (12) can be approximated by the expression above. This result is obtained by performing a series expansion of Euler beta and incomplete beta functions, specifically in the large- ε limit. The expansion assumes that the influence of the lower boundary is negligible. In the above, the symbol \simeq implies functional dependence of \bar{T} on ε . As this is functional dependence, it is not normalized in respect to L and x_0 (only terms involving ε are present).

Large ε limit implies that the drift term in the Fokker–Planck equation, Eq. 7, dominates the diffusion term. Stiff potential rendering the effects of a random force negligible. Consequently, in this limit, the nonlinearity of the diffusion coefficient can be safely ignored in the MFPT analysis. The functional dependence above, in its

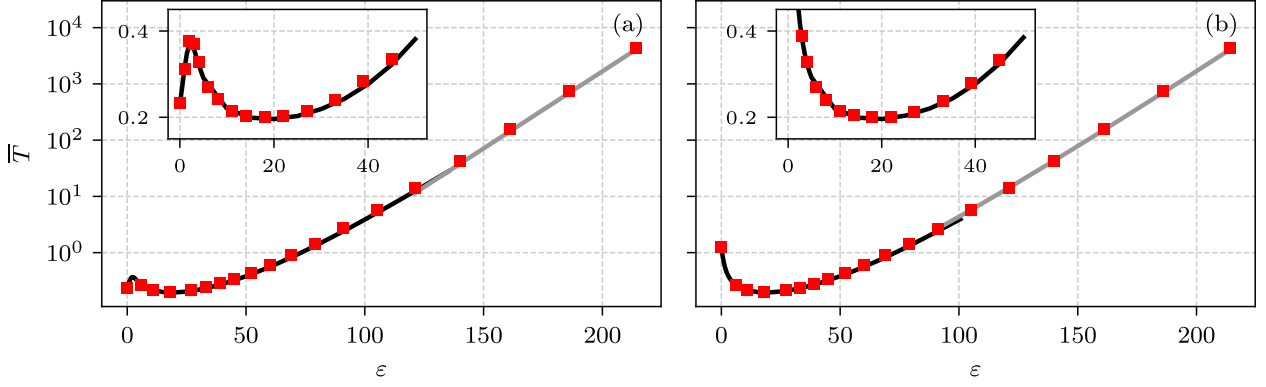


Figure 5: The mean first passage time \bar{T} dependence on the independent transition rate ε : (a) the case with absorbing boundary conditions at L and H , (b) the case with reflective boundary condition at L and absorbing boundary condition at H . The black curves correspond to Eq. (10) (for subfigure (a)) and Eq. (12) (for subfigure (b)), the gray curves follow Kramers' law, Eq. (28). The red squares represent estimates obtained by numerical simulation of Eq. (3) with $h = 1$ and $\varepsilon_0 = \varepsilon_1 = \varepsilon$. The insets show a more detailed dependence in the range of smaller ε . The boundary and initial conditions were set as follows $L = 0.03$, $H = 0.63$ and $x_0 = 0.23$.

purser form, i.e.,

$$\bar{T} \sim \varepsilon^{-3/2} e^{\varepsilon}, \quad (28)$$

matches Kramers' law for the MFPT in a stiff harmonic potential [81].

A comparison between the numerical simulations and analytical predictions in Fig. 5 confirms that the Kramers' law (gray curves) holds for both cases: with two absorbing boundary conditions (subfigure (a)) and with one reflective and one absorbing boundary condition (subfigure (b)). For small values of ε , the dependence of \bar{T} on ε is accurately described by Eq. (10) (black curve in subfigure (a)) and Eq. (12) (black curve in subfigure (b)). The insets in Fig. 5 provide a closer view of the dependence in the small ε value range.

4 Discussion

4.1 Numerical validation of analytical results and relation to other noisy voter models

We have derived exact analytical expressions for the mean first passage time (abbr. MFPT), \bar{T} , in the symmetric noisy voter model (i.e., with identical independent transition rates, $\varepsilon_0 = \varepsilon_1 = \varepsilon$). Eq. (10) corresponds to the case where both boundary conditions (located at L and H) are absorbing, while Eq. (10) applies when one of the boundaries is reflective (without loss of generality, we assume L is reflective). Unlike previous works, our expressions accommodate arbitrary placements of the initial (denoted by x_0) and boundary conditions, provided they satisfy a reasonable constraint $0 \leq L \leq x_0 \leq H \leq 1$. We have verified that the analytical results are in excellent quantitative agreement with numerical simulations.

In models involving imitation or herding behavior, the role of individualistic behavior is frequently underestimated [44]. Nevertheless, our research reveals that arbitrarily placed boundary conditions make \bar{T} dependence on x_0 asymmetric, and the presence of individualistic behavior can significantly exaggerate this asymmetry. When both boundaries are absorbing, asymmetry increases with ε (see Figs. 1, 3 (b) and 4): the location of \bar{T} maximum shifts toward the absorbing boundary that lies closer to the natural boundary, and the value of the maximum MFPT rises. In contrast, when one boundary is reflective, the qualitative asymmetry remains largely unchanged (see Fig. 2), while the overall MFPT decreases with increasing ε . Though, \bar{T} dependence on ε for fixed x_0 suggests that the behavior across a broader range of ε is more complex than it appears from the analysis of moderate ε (see Fig. 5). For extremely large ε , MFPT scales according to the Kramers' law for stiff

harmonic potential [81]. This contrasts with the asymptotic MFPT behavior found for the preferential voter model, which exhibits exponential decay [45].

We have also conducted a detailed analysis of the case with $\varepsilon = 0$, i.e., when the noisy voter model reduces to the original voter model on complete graph. We showed that the MFPT is symmetric only when the boundaries are placed symmetrically around the point where the diffusion is highest—at $x = \frac{1}{2}$ (see Fig. 3 (a)). This symmetry breaks down when the boundaries are not evenly placed around this point, leading to a directional bias in the MFPT due to the spatial variation in diffusivity (see Fig. 3 (b)). There are numerous previous works, which have considered mean consensus or mean polarization times for the original voter model and its minor modifications [52, 75–78]. Mean consensus times often correspond to the average transition time from a polarized state (e.g., $x = \frac{1}{2}$) to a complete consensus state (i.e., $x = 0$ or $x = 1$). Mean polarization times solve the opposite problem, i.e., finding the average time from consensus state to the polarized state. We show that these are just special cases of our more general MFPT expression, Eq. (16). Previous studies [52, 75–78] have established that these MFPTs exhibit a logarithmic dependence on the initial condition. Consistently, our expression reduces to a logarithmic dependence in the limiting case of $\varepsilon = 0$. However, in the general case, for $\varepsilon > 0$, general expressions involve special functions, which often are not as trivial to evaluate. We show that, for $\varepsilon = \frac{n}{2}$ with $n \in \mathbb{N}$, the MFPT can still be expressed in terms of trigonometric, logarithmic functions and polynomials. Previous work by Bhat and Redner [31] established this result for values up to $n = 4$. Our analysis extends these findings by revealing that such expressions arise from more general special functions, which we have carefully incorporated into our study.

4.2 Future Real-World Applications in Social and Physical Systems

In real-world social and political systems, boundary conditions are rarely symmetric. For example, proportional representation systems impose a lower vote threshold of about 4–5% for parliamentary entry [53], while a party is already considered successful with roughly 30–40% of the vote (far from the 95% upper bound assumed in symmetric models). Additional sociopolitical forces such as incumbency advantage [79], media influence, and strategic voting [80] further introduce asymmetry. Consequently, we focus on asymmetric boundary conditions when analyzing MFPT, as this better reflects threshold-based decision processes in social systems.

A key theoretical contribution of this work is the exact analytical solution of the ordinary differential equation (9), expressed in terms of the incomplete beta function and the Meijer G -function, as presented in B (Eq. (66)). To the best of our knowledge, this solution is both unique and previously undocumented in the physical or social science literature. Additionally, Eqs. (10) and Eqs. (12), which incorporate arbitrary boundary placements, represent a novel generalization of earlier models. These expressions extend prior studies by accommodating non-symmetric and mixed boundary conditions, offering a more flexible and realistic framework for analyzing MFPT in noisy voter dynamics. Prior studies often impose symmetric boundaries to simplify analysis [37–40], but this assumption is overly restrictive given the inherently uneven expectations in systems with thresholds. The noisy voter model is well suited for social applications such as opinion dynamics. For example, a party’s stable core support may be modeled by a reflective boundary at low x , while a funding threshold is represented by an absorbing boundary. Thus, our analytical MFPT result is directly actionable for quantifying how long a new political party is expected to take to reach viability under stochastic dynamics.

Beyond social systems, the model also has relevance in physical contexts. It has been shown that the stochastic differential equation (3) can be approximated by heterogeneous diffusion processes (abbr. HDPs) [82], which describe particle diffusion in systems with temperature gradients [83, 84] and external potentials [85]. These connections suggest potential applications in anomalous diffusion [83, 85], power-law statistics [84, 86], and $1/f$ noise [63, 87]. Conversely, HDPs can also be approximated by voter models, allowing the MFPT expressions derived here to serve as useful estimates in physical systems. Anomalous diffusion has also been observed in social dynamics, such as human movement intermittency [88] and parliamentary presence [28, 89]. Nonlinear transformations of the noisy voter model can mimic statistical properties of fractional Brownian motion [82, 90],

a standard model for persistent and anti-persistent diffusion and long-range memory [91]. This research may therefore be useful for studying persistence and anti-persistence in various time-series data. In the case of time-dependent herding, approximate formulas for the first-passage time distribution have been obtained under restrictive conditions, such as small signal intensity and neglecting one boundary [78]. Thus the chosen direction, toward more realistic and flexible modeling of asymmetry and time dependence, appears especially promising, as it builds directly on the analytical foundations established in this work and opens pathways for broader applications.

Looking ahead, we plan to extend this framework to asymmetric noisy voter models, particularly in regimes with asymmetric transition rates. These models are analytically challenging but offer rich dynamics that merit further exploration. We also recognize the potential for incorporating time-dependent parameters and boundary conditions to model adaptive or externally driven systems. While exact solutions may not be feasible in such cases, approximate methods and numerical simulations could provide valuable insights.

5 Conclusions

We derived exact analytical expressions for the mean first passage time (abbr. MFPT) in the symmetric noisy voter model with identical transition rates. These results apply to both absorbing and mixed boundary conditions and allow for arbitrary placements of the initial and boundary states within the interval $[0, 1]$. Our analytical predictions show excellent agreement with numerical simulations. Our analysis highlights how individualistic behavior and asymmetric boundary placement significantly influence MFPT. These factors introduce directional bias and shift the location of the maximum MFPT. For large noise levels (ε), the MFPT scales according to Kramers' law, in contrast to the exponential decay observed in preferential voter models.

In absence of individualistic behaviour ($\varepsilon = 0$), the model reduces to the classical voter model, where MFPT exhibits a logarithmic dependence on the initial condition. Symmetry in MFPT is preserved only when boundaries are placed evenly around $x = \frac{1}{2}$, the point of highest diffusivity. Otherwise, asymmetry emerges due to spatial variation in diffusion. Consensus and polarization times, widely studied in earlier works, emerge as special cases of our more general MFPT formulation. For specific values of $\varepsilon = \frac{n}{2}$, MFPTs can be expressed using elementary functions, extending previous results to broader parameter ranges. These expressions offer practical tools for analyzing MFPTs in heterogeneous diffusion processes, which can be approximated by voter models and vice versa.

A central novelty of our study is the general solution to ordinary differential equation (9), presented in B (Eq. (66)), which involves the incomplete beta function and the Meijer G -function. To the best of our knowledge, this solution is both unique and previously undocumented in physical or social science literature. Additionally, the MFPT results in Eqs. (10) and Eqs. (12), which explicitly incorporate boundary conditions, represent a significant generalization of earlier models and introduce new analytical structures to the study of stochastic dynamics.

Finally, we acknowledge that model simplifications (such as symmetric transition rates and fixed boundaries) affect the generality of the results. However, these choices are necessary to obtain tractable analytical solutions. Future work may explore more complex scenarios, including asymmetric time-dependent transition rates, external perturbations, and dynamic boundary conditions.

References

- [1] R.-T. Qiu, W.-S. Dai, M. Xie, Mean first-passage time of quantum transition processes, *Physica A: Statistical Mechanics and its Applications* 391 (20) (2012) 4748–4755. doi:10.1016/j.physa.2012.05.050.
- [2] J. Wu, R. J. Silbey, J. Cao, Generic mechanism of optimal energy transfer efficiency: A scaling theory of the mean first-passage time in exciton systems, *Phys. Rev. Lett.* 110 (20) (2013) 200402. doi:10.1103/physrevlett.110.200402.

- [3] H. Friedman, D. A. Kessler, E. Barkai, Quantum renewal equation for the first detection time of a quantum walk, *Journal of Physics A: Mathematical and Theoretical* 50 (4) (2016) 04LT01. doi:10.1088/1751-8121/aa5191.
- [4] Q. Liu, R. Yin, K. Ziegler, E. Barkai, Quantum walks: The mean first detected transition time, *Phys. Rev. Res.* 2 (2020) 033113. doi:10.1103/PhysRevResearch.2.033113.
- [5] Y. Hasegawa, Thermodynamic uncertainty relation for quantum first-passage processes, *Phys. Rev. E* 105 (2022) 044127. doi:10.1103/PhysRevE.105.044127.
- [6] M. Kulkarni, S. N. Majumdar, First detection probability in quantum resetting via random projective measurements, *Journal of Physics A: Mathematical and Theoretical* 56 (38) (2023) 385003. doi:10.1088/1751-8121/acf103.
- [7] M. J. Kewming, A. Kiely, S. Campbell, G. T. Landi, First passage times for continuous quantum measurement currents, *Phys. Rev. A* 109 (5) (2024) 1050202. doi:10.1103/PhysRevA.109.L050202.
- [8] R. Roy, R. Short, J. Durnin, L. Mandel, First-passage-time distributions under the influence of quantum fluctuations in a laser, *Phys. Rev. Lett.* 45 (18) (1980) 1486–1490. doi:10.1103/physrevlett.45.1486.
- [9] L. Cao, D.-j. Wu, Mean first-passage time of laser phase in a single-mode laser, *Physics Letters A* 283 (5-6) (2001) 313–318. doi:10.1016/s0375-9601(01)00262-6.
- [10] N. Kalantar, D. Segal, Mean first-passage time and steady-state transfer rate in classical chains, *The Journal of Physical Chemistry C* 123 (2) (2019) 1021–1031. doi:10.1021/acs.jpcc.8b08874.
- [11] R. J. Preston, M. F. Gelin, D. S. Kosov, First-passage time theory of activated rate chemical processes in electronic molecular junctions, *The Journal of Chemical Physics* 154 (11) (2021) 114108. doi:10.1063/5.0045652.
- [12] S. Ravichandir, B. Valecha, P. L. Muzzeddu, J.-U. Sommer, A. Sharma, Transport of partially active polymers in chemical gradients, *Soft Matter* 21 (10) (2025) 1835–1840. doi:10.1039/D4SM01357C.
- [13] N. F. Polizzi, M. J. Therien, D. N. Beratan, Mean first-passage times in biology, *Israel Journal of Chemistry* 56 (9-10) (2016) 816–824. doi:10.1002/ijch.201600040.
- [14] Y. Zhang, O. K. Dudko, First-passage processes in the genome, *Annual Review of Biophysics* 45 (1) (2016) 117–134. doi:10.1146/annurev-biophys-062215-010925.
- [15] V. Singh, P. Biswas, Estimating the mean first passage time of protein misfolding, *Phys. Chem. Chem. Phys.* 20 (2018) 5692–5698. doi:10.1039/C7CP06918A.
- [16] Y. Zhou, J. Du, The mean first passage time in an energy-diffusion controlled regime with power-law distributions, *Journal of Statistical Mechanics: Theory and Experiment* 2013 (11) (2013) P11005. doi:10.1088/1742-5468/2013/11/p11005.
- [17] J.-H. Kim, H. Lee, S. Song, H. R. Koh, J. Sung, Observation time dependent mean first passage time of diffusion and subdiffusion processes, *Journal of Statistical Mechanics: Theory and Experiment* 2020 (3) (2020) 033204. doi:10.1088/1742-5468/ab6f62.
- [18] D. Grebenkov, R. Metzler, G. Oshanin (Eds.), *Target Search Problems*, 1st Edition, Springer Nature Switzerland, 2024. doi:10.1007/978-3-031-67802-8.
- [19] H. Risken, *The Fokker–Planck Equation: Methods of Solution and Applications*, Springer Berlin Heidelberg, Berlin, 1996. doi:10.1007/978-3-642-61544-3.
- [20] C. W. Gardiner, *Handbook of stochastic methods for Physics, Chemistry and the Natural Sciences*, 4th Edition, Springer complexity, Springer-Verlag, Berlin, 2004, includes bibliographical references and index. - Previous ed.: 2004.
- [21] A. N. Borodin, P. Salminen, *Handbook of Brownian Motion - Facts and Formulae*, 2nd Edition, Birkhäuser Basel, 2002. doi:10.1007/978-3-0348-8163-0.
- [22] A. Kononovicius, V. Gontis, Approximation of the first passage time distribution for the birth-death processes, *Journal of Statistical Mechanics* 2019 (2019) 073402. doi:10.1088/1742-5468/ab2709.
- [23] A. Bassolas, V. Nicosia, First-passage times to quantify and compare structural correlations and heterogeneity in complex systems, *Communications Physics* 4 (1) (Apr. 2021). doi:10.1038/s42005-021-00580-w.
- [24] R. Kutner, M. Ausloos, D. Grech, T. Di Matteo, C. Schinckus, H. Eugene Stanley, *Econophysics and sociophysics: Their milestones & challenges*, *Physica A* 516 (2019) 240–253. doi:10.1016/j.physa.2018.10.019.
- [25] H. Hu, W. Chen, Y. Hu, Opinion dynamics in social networks under the influence of mass media, *Applied Mathematics and Computation* 482 (2024) 128976. doi:10.1016/j.amc.2024.128976.
- [26] J. Fernández-Gracia, K. Suchecki, J. J. Ramasco, M. San Miguel, V. M. Eguíluz, Is the voter model a model for voters?, *Phys. Rev. Lett.* 112 (15) (2014) 158701. doi:10.1103/physrevlett.112.158701.
- [27] D. Braha, M. A. M. de Aguiar, Voting contagion: Modeling and analysis of a century of u.s. presidential elections, *PLOS ONE* 12 (5) (2017) e0177970. doi:10.1371/journal.pone.0177970.
- [28] A. Kononovicius, Empirical analysis and agent-based modeling of the lithuanian parliamentary elections, *Complexity* 2017 (2017) 1–15. doi:10.1155/2017/7354642.
- [29] S. Marmani, V. Ficcadenti, P. Kaur, G. Dhesi, Entropic analysis of votes expressed in Italian elections between 1948 and 2018, *Entropy* 22 (2020) 523. doi:10.3390/e22050523.

- [30] A. Baronchelli, The emergence of consensus: a primer, *Royal Society Open Science* 5 (2018) 172189. doi:10.1098/rsos.172189.
- [31] D. Bhat, S. Redner, Polarization and consensus by opposing external sources, *Journal of Statistical Mechanics: Theory and Experiment* 2020 (1) (2020) 013402. doi:10.1088/1742-5468/ab6094.
- [32] T. Fushimi, K. Saito, M. Kimura, H. Motoda, K. Ohara, Finding relation between pagerank and voter model, in: B.-H. Kang, D. Richards (Eds.), *Knowledge Management and Acquisition for Smart Systems and Services*, Springer Berlin Heidelberg, Berlin, Heidelberg, 2010, pp. 208–222. doi:10.1007/978-3-642-15037-1_18.
- [33] M. Kimura, K. Saito, K. Ohara, H. Motoda, Detecting anti-majority opinionists using value-weighted mixture voter model, in: T. Elomaa, J. Hollmén, H. Mannila (Eds.), *Discovery Science*, Springer Berlin Heidelberg, Berlin, Heidelberg, 2011, pp. 150–164. doi:10.1007/978-3-642-24477-3_14.
- [34] M. Kimura, K. Saito, K. Ohara, H. Motoda, Learning to predict opinion share and detect anti-majority opinionists in social networks, *Journal of Intelligent Information Systems* 41 (1) (2012) 5–37. doi:10.1007/s10844-012-0222-7.
- [35] K. Rawal, A. Khan, Maximizing contrasting opinions in signed social networks, *2019 IEEE International Conference on Big Data (Big Data)* (2019) 1203–1210. doi:10.1109/BigData47090.2019.9005619.
- [36] Q. He, X. Wang, M. Huang, B. Yi, Multi-stage opinion maximization in social networks, *Neural Computing and Applications* 33 (19) (2021) 12367–12380. doi:10.1007/s00521-021-05840-y.
- [37] C. Castellano, S. Fortunato, V. Loreto, Statistical physics of social dynamics, *Rev. Mod. Phys.* 81 (2009) 591–646. doi:10.1103/RevModPhys.81.591.
- [38] A. Jędrzejewski, K. Sznajd-Weron, Statistical physics of opinion formation: Is it a SPOOF?, *C. R. Phys.* 20 (4) (2019) 244–261. doi:10.1016/j.crhy.2019.05.002.
- [39] H. Noorazar, Recent advances in opinion propagation dynamics, *The European Physical Journal Plus* 135 (2020) 521. doi:10.1140/epjp/s13360-020-00541-2.
- [40] S. Redner, Reality inspired voter models: a mini-review, *C. R. Phys.* 20 (4) (2019) 275–292. doi:10.1016/j.crhy.2019.05.004.
- [41] N. Masuda, N. Gibert, S. Redner, Heterogeneous voter models, *Phys. Rev. E* 82 (2010) 010103. doi:10.1103/PhysRevE.82.010103.
- [42] L. Rozanova, M. Boguñá, Dynamical properties of the herding voter model with and without noise, *Phys. Rev. E* 96 (2017) 012310. doi:10.1103/PhysRevE.96.012310.
- [43] F. Perachia, P. Román, S. A. Menchón, Noisy voter model: Explicit expressions for finite system size, *Phys. Rev. E* 106 (2022) 054155. doi:10.1103/PhysRevE.106.054155.
- [44] S. Kudtarkar, First-passage distributions of an asymmetric noisy voter model, *Phys. Rev. E* 109 (2) (2024) 024139. doi:10.1103/PhysRevE.109.024139.
- [45] Z. Q. Lee, W.-J. Hsu, M. Lin, How well-connected individuals help spread influences – analyses based on preferential voter model, in: *2012 IEEE/ACM International Conference on Advances in Social Networks Analysis and Mining, IEEE, 2012*, pp. 674–678. doi:10.1109/asonam.2012.112.
- [46] A. Kirman, Ants, rationality, and recruitment, *The Quarterly Journal of Economics* 108 (1) (1993) 137–156. doi:10.2307/2118498.
- [47] S. Alfarano, T. Lux, F. Wagner, Time variation of higher moments in a financial market with heterogeneous agents: An analytical approach, *J. Econ. Dyn. Control* 32 (2008) 101–136. doi:10.1016/j.jedc.2006.12.014.
- [48] A. Kononovicius, V. Gontis, Agent based reasoning for the non-linear stochastic models of long-range memory, *Physica A: Statistical Mechanics and its Applications* 391 (4) (2012) 1309–1314. doi:10.1016/j.physa.2011.08.061.
- [49] A. Kononovicius, J. Ruseckas, Order book model with herding behavior exhibiting long-range memory, *Physica A* 525 (2019) 171–191. doi:10.1016/j.physa.2019.03.059.
- [50] H. Chen, G. Li, F. Huang, First passage in discrete-time absorbing markov chains under stochastic resetting, *Journal of Physics A: Mathematical and Theoretical* 55 (38) (2022) 384005. doi:10.1088/1751-8121/ac87dd.
- [51] R. Martínez-García, F. Vazquez, C. López, M. A. Muñoz, Temporal disorder in up-down symmetric systems, *Phys. Rev. E* 85 (2012) 051125. doi:10.1103/PhysRevE.85.051125.
- [52] S. Redner, *A Guide to First-Passage Processes*, Cambridge University Press, Cambridge, 2001. doi:10.1017/cbo9780511606014.
- [53] M. Gallagher, P. Mitchell, *The Politics of Electoral Systems*, Oxford University Press, 2005. doi:10.1093/0199257566.001.0001.
- [54] P. Clifford, A. Sudbury, A model for spatial conflict, *Biometrika* 60 (1973) 581–588. doi:10.1093/biomet/60.3.581.
- [55] T. M. Liggett, *Stochastic Interacting Systems: Contact, Voter and Exclusion Processes*, Springer Berlin Heidelberg, 1999. doi:10.1007/978-3-662-03990-8.
- [56] R. H. Willis, Conformity, independence, and anticonformity, *Human Relations* 18 (4) (1965) 373–388. doi:10.1177/001872676501800406.

- [57] P. Nail, K. Sznajd-Weron, The diamond model of social response within an agent-based approach, *Acta Physica Polonica A* 129 (5) (2016) 1050–1054. doi:10.12693/aphyspola.129.1050.
- [58] B. L. Granovsky, N. Madras, The noisy voter model, *Stochastic Processes and their Applications* 55 (1) (1995) 23–43. doi:10.1016/0304-4149(94)00035-r.
- [59] J. Ruseckas, B. Kaulakys, V. Gontis, Herding model and $1/f$ noise, *EPL* 96 (6) (2011) 60007. doi:10.1209/0295-5075/96/60007.
- [60] N. G. van Kampen, *Stochastic process in physics and chemistry*, North Holland, Amsterdam, 2007. doi:10.1016/B978-0-444-52965-7.X5000-4.
- [61] S. Mori, M. Hisakado, K. Nakayama, Voter model on networks and the multivariate beta distribution, *Phys. Rev. E* 99 (2019) 052307. doi:10.1103/PhysRevE.99.052307.
- [62] P. E. Kloeden, E. Platen, *Numerical Solution of Stochastic Differential Equations*, Springer Berlin Heidelberg, Berlin, 1992. doi:10.1007/978-3-662-12616-5.
- [63] J. Ruseckas, R. Kazakevičius, B. Kaulakys, $1/f$ noise from point process and time-subordinated langevin equations, *Journal of Statistical Mechanics: Theory and Experiment* 2016 (5) (2016) 054022. doi:10.1088/1742-5468/2016/05/054022.
- [64] URL <https://github.com/akononovicius/mfpt-symmetric-noisy-voter-model>
- [65] A. Kononovicius, R. Astrauskas, M. Radavičius, F. Ivanauskas, Delayed interactions in the noisy voter model through the periodic polling mechanism, *Physica A: Statistical Mechanics and its Applications* 652 (2024) 130062. doi:10.1016/j.physa.2024.130062.
- [66] J. Grasman, O. A. van Herwaarden, *Asymptotic Methods for the Fokker–Planck Equation and the Exit Problem in Applications*, 1st Edition, Springer Series in Synergetics, Springer Berlin Heidelberg, 1999, springer Book Archive, Copyright Springer-Verlag Berlin Heidelberg 1999. doi:10.1007/978-3-662-03857-4.
- [67] B. Lindner, Moments of the first passage time under external driving, *Journal of Statistical Physics* 117 (3) (2004) 703–737. doi:10.1007/s10955-004-2269-5.
- [68] C. A. Moreira, D. M. Schneider, M. A. M. de Aguiar, Binary dynamics on star networks under external perturbations, *Phys. Rev. E* 92 (4) (2015) 042812. doi:10.1103/physreve.92.042812.
- [69] E. Urdapilleta, First-passage-time statistics of a brownian particle driven by an arbitrary unidimensional potential with a superimposed exponential time-dependent drift, *Journal of Physics A: Mathematical and Theoretical* 48 (50) (2015) 505001. doi:10.1088/1751-8113/48/50/505001.
- [70] S. Ahmad, I. Nayak, A. Bansal, A. Nandi, D. Das, First passage of a particle in a potential under stochastic resetting: A vanishing transition of optimal resetting rate, *Phys. Rev. E* 99 (2019) 022130. doi:10.1103/PhysRevE.99.022130.
- [71] M. Mobilia, A. Petersen, S. Redner, On the role of zealotry in the voter model, *J. Stat. Mech.* 2007 (08) (2007) P08029. doi:10.1088/1742-5468/2007/08/p08029.
- [72] S. Galam, F. Jacobs, The role of inflexible minorities in the breaking of democratic opinion dynamics, *Physica A* 381 (2007) 366–376. doi:10.1016/j.physa.2007.03.034.
- [73] A. Kononovicius, V. Gontis, Control of the socio-economic systems using herding interactions, *Physica A: Statistical Mechanics and its Applications* 405 (2014) 80–84. doi:10.1016/j.physa.2014.03.003.
- [74] N. Khalil, M. San Miguel, R. Toral, Zealots in the mean-field noisy voter model, *Phys. Rev. E* 97 (2018) 012310. doi:10.1103/PhysRevE.97.012310.
- [75] V. Sood, S. Redner, Voter model on heterogeneous graphs, *Phys. Rev. Lett.* 94 (2005) 178701. doi:10.1103/PhysRevLett.94.178701.
- [76] V. Sood, T. Antal, S. Redner, Voter models on heterogeneous networks, *Phys. Rev. E* 77 (2008) 041121. doi:10.1103/PhysRevE.77.041121.
- [77] G. J. Baxter, A voter model with time dependent flip rates, *Journal of Statistical Mechanics: Theory and Experiment* 2011 (09) (2011) P09005. doi:10.1088/1742-5468/2011/09/P09005.
- [78] A. Mukhopadhyay, R. R. Mazumdar, R. Roy, Voter and majority dynamics with biased and stubborn agents, *Journal of Statistical Physics* 181 (4) (2020) 1239–1265. doi:10.1007/s10955-020-02625-w.
- [79] R. S. Erikson, R. Titiunik, Using regression discontinuity to uncover the personal incumbency advantage, *Quarterly Journal of Political Science* 10 (1) (2015) 101–119. doi:10.1561/100.00013137.
- [80] J. Cohen, Y. Tsfati, The influence of presumed media influence on strategic voting, *Communication Research* 36 (3) (2009) 359–378. doi:10.1177/0093650209333026.
- [81] W. K. Kim, R. R. Netz, The mean shape of transition and first-passage paths, *The Journal of Chemical Physics* 143 (22) (2015) 224108. doi:10.1063/1.4936408.
- [82] R. Kazakevičius, A. Kononovicius, Anomalous diffusion in nonlinear transformations of the noisy voter model, *Phys. Rev. E* 103 (2021) 032154. doi:10.1103/PhysRevE.103.032154.
- [83] A. G. Cherstvy, A. V. Chechkin, R. Metzler, Anomalous diffusion and ergodicity breaking in heterogeneous diffusion processes, *New Journal of Physics* 15 (8) (2013) 083039. doi:10.1088/1367-2630/15/8/083039.

- [84] R. Kazakevičius, J. Ruseckas, Power law statistics in the velocity fluctuations of brownian particle in inhomogeneous media and driven by colored noise, *Journal of Statistical Mechanics: Theory and Experiment* 2015 (2015) P02021. doi:10.1088/1742-5468/2015/02/P02021.
- [85] R. Kazakevičius, J. Ruseckas, Influence of external potentials on heterogeneous diffusion processes, *Phys. Rev. E* 94 (3) (2016) 032109. doi:10.1103/PhysRevE.94.032109.
- [86] R. Kazakevičius, J. Ruseckas, Power-law statistics from nonlinear stochastic differential equations driven by lévy stable noise, *Chaos, Solitons & Fractals* 81 (2015) 432–442. doi:10.1016/j.chaos.2015.08.024.
- [87] R. Kazakevičius, J. Ruseckas, Lévy flights in inhomogeneous environments and 1/f noise, *Physica A: Statistical Mechanics and its Applications* 411 (2014) 95–103. doi:10.1016/j.physa.2014.06.020.
- [88] X. Luo, X. Dai, Y. Li, J. Song, W. Fan, Anomalous diffusions of the composite processes: Generalized lévy walk with jumps or rests, *Physica A: Statistical Mechanics and its Applications* 665 (2025) 130503. doi:10.1016/j.physa.2025.130503.
- [89] A. Kononovicius, Noisy voter model for the anomalous diffusion of parliamentary presence, *Journal of Statistical Mechanics: Theory and Experiment* 2020 (6) (2020) 063405. doi:10.1088/1742-5468/ab8c39.
- [90] A. Kononovicius, R. Kazakevičius, B. Kaulakys, Resemblance of the power-law scaling behavior of a non-Markovian and nonlinear point processes, *Chaos Soliton. Fract.* 162 (2022) 112508. doi:https://doi.org/10.1016/j.chaos.2022.112508.
- [91] O. C. Ibe, *Markov Processes for Stochastic Modeling*, Elsevier, 2013. doi:10.1016/C2012-0-06106-6.
- [92] V. Gontis, A. Kononovicius, Bessel-like birth-death process, *Physica A* 540 (2020) 123119. doi:10.1016/j.physa.2019.123119.
- [93] R. Kazakevičius, A. Kononovicius, Anomalous diffusion and long-range memory in the scaled voter model, *Phys. Rev. E* 107 (2) (2023) 024106. doi:10.1103/physreve.107.024106.

A Derivation of the ordinary differential equation for the mean first passage time

Here, we derive an ordinary differential equation for calculating the mean first-passage time from the Fokker–Planck equation in the single-variable case. For the multivariable case, a general framework for deriving MFPT ODEs can be found in Refs. [19, 20, 66].

The survival probability—the probability that a particle remains within the interval $x \in [a, b]$ up to time t (smaller or equal to first passage time), without having reached the interval boundary—is given by:

$$\text{Prob}(T \geq t) = G(x_0, t) = \int_a^b P(x, t | x_0, 0) dx, \quad (29)$$

where, $P(x, t | x_0, 0)$ is the transition probability density, i.e., the conditional probability that a particle starting at position x_0 at time zero is found at position x at time t . The probability that the particle has exited the domain $x \in [a, b]$ by time t is given by:

$$\text{Prob}(T \leq t) = 1 - \text{Prob}(T \geq t) = 1 - G(x_0, t). \quad (30)$$

The FPTD, denoted $p_T(T)$, describes the probability that the particle crosses either boundary a or b for the first time within the infinitesimal interval $(t, t + dt)$. It is given by the negative time derivative of the survival probability:

$$p_T(t) = \frac{\partial}{\partial t} \text{Prob}(T \leq t) = \frac{\partial}{\partial t} (1 - G(x_0, t)) = -\frac{\partial}{\partial t} G(x_0, t). \quad (31)$$

The MFPT is defined as the expected value of the first-passage time:

$$\bar{T}(x_0) = \int_0^\infty t p_T(t) dt = - \int_0^\infty t \frac{\partial}{\partial t} G(x_0, t) dt. \quad (32)$$

To evaluate the MFPT, we consider the integral:

$$I = - \int_0^\infty t \frac{\partial}{\partial t} G(x_0, t) dt. \quad (33)$$

Let us apply the integration by parts using the standard formula:

$$\int u dv = uv - \int v du. \quad (34)$$

Here, let us choose

$$u = t \Rightarrow du = dt, \quad dv = \frac{\partial}{\partial t} G(x_0, t) dt \Rightarrow v = G(x_0, t). \quad (35)$$

Substituting Eqs. (34) and (35) into the formula (33), we obtain:

$$I = - \int_0^\infty t dG(x_0, t) = - \left[tG(x_0, t) \Big|_0^\infty - \int_0^\infty G(x_0, t) dt \right]. \quad (36)$$

By definition, $G(x_0, 0) = 1$ for all $x_0 \in [a, b]$. This immediately implies that $tG(x_0, t) \rightarrow 0$ as $t \rightarrow 0$, since the factor of t vanishes. To ensure that the boundary term in an integration by parts vanishes at the upper limit, we require $\lim_{t \rightarrow \infty} tG(x_0, t) = 0$. This condition holds if $G(x_0, t)$ decays faster than $\frac{1}{t}$ as $t \rightarrow \infty$. For instance, this is satisfied when $G(x_0, t) \sim e^{-t}$ or $G(x_0, t) \sim \frac{1}{t^\gamma}$ with $\gamma > 1$. Assuming such decay, the boundary term $tG(x_0, t) \Big|_0^\infty$ vanishes, and we are left with:

$$I = - \int_0^\infty t \frac{\partial}{\partial t} G(x_0, t) dt = \int_0^\infty G(x_0, t) dt. \quad (37)$$

Comparing formulas (32) and (37), we find the relationship between the MFPT and the survival probability:

$$\bar{T}(x_0) = - \int_0^\infty t \frac{\partial}{\partial t} G(x_0, t) dt = \int_0^\infty G(x_0, t) dt. \quad (38)$$

If the system is governed by the Fokker–Planck equation

$$\frac{\partial}{\partial t} P(x, t | x_0, 0) = -\frac{\partial}{\partial x} A(x) P(x, t | x_0, 0) + \frac{1}{2} \frac{\partial^2}{\partial x^2} B(x) P(x, t | x_0, 0), \quad (39)$$

and the process is time-homogeneous—that is, $P(x, t | x_0, 0) = P(x, 0 | x_0, -t)$, then the corresponding time-backward Fokker–Planck equation takes the form

$$\frac{\partial}{\partial t} P(x, t | x_0, 0) = A(x_0) \frac{\partial}{\partial x_0} P(x, t | x_0, 0) + \frac{1}{2} B(x_0) \frac{\partial^2}{\partial x_0^2} P(x, t | x_0, 0). \quad (40)$$

To relate this to the survival probability, we integrate both sides of the time-backward equation (40) over $x \in [a, b]$:

$$\frac{\partial}{\partial t} \int_a^b P(x, t | x_0, 0) dx = A(x_0) \frac{\partial}{\partial x_0} \int_a^b P(x, t | x_0, 0) dx + \frac{1}{2} B(x_0) \frac{\partial^2}{\partial x_0^2} \int_a^b P(x, t | x_0, 0) dx. \quad (41)$$

Recognizing that the integral on the left-hand side corresponds to the survival probability $G(x_0, t)$, as defined in Eq. (29), we can rewrite the equation as:

$$\frac{\partial}{\partial t} G(x_0, t) = A(x_0) \frac{\partial}{\partial x_0} G(x_0, t) + \frac{1}{2} B(x_0) \frac{\partial^2}{\partial x_0^2} G(x_0, t). \quad (42)$$

This shows that the survival probability $G(x_0, t)$ satisfies the time-backward Fokker–Planck equation and can be obtained by directly solving it. Next, we integrate both sides of this equation with respect to t from 0 to ∞

$$\int_0^\infty \frac{\partial}{\partial t} G(x_0, t) dt = A(x_0) \frac{\partial}{\partial x_0} \int_0^\infty G(x_0, t) dt + \frac{1}{2} B(x_0) \frac{\partial^2}{\partial x_0^2} \int_0^\infty G(x_0, t) dt, \quad (43)$$

Recalling the previously obtained relation between the MFPT and the survival probability, Eq. (29), we see that the equation above is

$$G(x_0, \infty) - G(x_0, 0) = A(x_0) \frac{d}{dx_0} \bar{T}(x_0) + \frac{1}{2} B(x_0) \frac{d^2}{dx_0^2} \bar{T}(x_0). \quad (44)$$

We assume that $G(x, \infty) = 0$, since any particle is eventually absorbed. From the initial condition $p(x, 0 | x_0, 0) = \delta(x_0 - x)$, it follows that $G(x, 0) = 1$ for $x \in [a, b]$. Substituting these values into the Eq. (44) yields:

$$\frac{1}{2} B(x_0) \frac{d^2}{dx_0^2} \bar{T}(x_0) + A(x_0) \frac{d}{dx_0} \bar{T}(x_0) = -1, \quad (45)$$

which is the ODE that arises from the time-backward Fokker–Planck equation for the MFPT, Eq. (40).

B Solution of the ordinary differential equation governing the mean first-passage time

We now solve the ODE that determines the MFPT. The symmetric noisy voter model is governed by the time-backward Fokker–Planck equation, Eq. (8). Combining this with the previously established relation given by Eq. (45) yields the following ODE for the MFPT:

$$\frac{d^2}{dx_0^2} \bar{T}(x_0) + \varepsilon \frac{1 - 2x_0}{x_0(1 - x_0)} \frac{d}{dx_0} \bar{T}(x_0) = -\frac{1}{x_0(1 - x_0)}. \quad (46)$$

First, we find the general solution. Next, we incorporate the effects of the boundary conditions. The complementary (homogeneous) ODE corresponding to the equation above is:

$$\frac{d^2}{dx_0^2} \bar{T}_c(x_0) + \varepsilon \frac{1 - 2x_0}{x_0(1 - x_0)} \frac{d}{dx_0} \bar{T}_c(x_0) = 0. \quad (47)$$

The subscript c on \bar{T}_c indicates that this is the complementary solution. By introducing a new variable

$$\nu(x_0) = \frac{d\bar{T}_c}{dx_0}, \quad (48)$$

we can reduce the second-order ODE mentioned above to a first-order ODE

$$\frac{1}{\nu(x_0)} d\nu(x_0) = -\varepsilon \frac{1 - 2x_0}{x_0(1 - x_0)} dx_0, \quad (49)$$

by integrating both sides of Eq. (49), we obtain the following equality:

$$\ln(\nu(x_0)) = -\varepsilon (\ln(1 - x_0) + \ln(x_0)) + \ln(c_1). \quad (50)$$

By the exponentiation of the both sides of the above equality to eliminate the logarithm, we express the variable $\nu(x_0)$ as:

$$\nu(x_0) = \frac{c_1}{x_0^\varepsilon (1 - x_0)^\varepsilon}. \quad (51)$$

By integrating Eq. (48) with respect to x_0 , we find that the complementary solution can be expressed in terms of $\nu(x_0)$:

$$\bar{T}_c(x_0) = c_2 - c_1 \int \nu(x_0) dx_0. \quad (52)$$

The integral on the right-hand side of \bar{T}_c can be expressed by using incomplete beta function

$$\beta_z(a, b) = \int_0^z r^{a-1} (1-r)^{b-1} dr, \quad (53)$$

using this, the solution of the complementary ODE (46) is:

$$\bar{T}_c(x_0) = c_2 - c_1 \beta_{1-x_0}(1-\varepsilon, 1-\varepsilon). \quad (54)$$

Here, $\beta_{1-x_0}(1-\varepsilon, 1-\varepsilon)$ denotes the incomplete beta function. While this function has singularities at integer values of ε , as we will demonstrate later, the integral in Eq. (52) can still be evaluated even when ε takes integer values.

To find a particular solution \bar{T}_p based on the complementary solution \bar{T}_c , we apply the variation of parameters method. According to this method, if the complementary solution of the ODE is given by:

$$\bar{T}_c(x_0) = c_1 s_1(x_0) + c_2 s_2(x_0), \quad (55)$$

The particular solution can then be written as:

$$\bar{T}_p(x_0) = s_2(x_0) \int s_1(x_0) \frac{r(x_0)}{w(x_0)} dx_0 - s_1(x_0) \int s_2(x_0) \frac{r(x_0)}{w(x_0)} dx_0. \quad (56)$$

Here, $w(x_0)$ denotes

$$w(x_0) = s_1(x_0) \frac{d}{dx_0} s_2(x_0) - s_2(x_0) \frac{d}{dx_0} s_1(x_0), \quad (57)$$

where $r(x_0)$ represents the inhomogeneous part of the ODE. From ODE (46), it follows that in our case:

$$r(x_0) = -\frac{1}{x_0(1-x_0)}. \quad (58)$$

By comparing Eq. (54) with Eq. (55), we observe that

$$s_1(x_0) = -\beta_{1-x_0}(1-\varepsilon, 1-\varepsilon), \quad (59)$$

and

$$s_2(x_0) = 1. \quad (60)$$

By substituting Eqs. (58), (59), and (60) into Eq. (56), we obtain the particular solution:

$$\bar{T}_p(x_0) = -\beta_{1-x_0}(1-\varepsilon, 1-\varepsilon) \beta_{1-x_0}(\varepsilon, \varepsilon) - \int ((1-x_0)x_0)^{\varepsilon-1} \beta_{1-x_0}(1-\varepsilon, 1-\varepsilon) dx_0, \quad (61)$$

in the integral form. The integral on the right-hand side of Eq. (61) can be evaluated using the relation between the incomplete beta function $B_z(a, b)$ and the hypergeometric function, defined as:

$$\beta_z(a, b) = \left(\frac{z^a}{a}\right) {}_2F_1(a, 1-b; a+1; z), \quad (62)$$

The function ${}_2F_1(a, 1-b; a+1; z)$ is a Gauss hypergeometric function, defined by the series:

$${}_2F_1(a, 1-b; a+1; z) = \sum_{k=0}^{\infty} \frac{(a)_k (1-b)_k}{(a+1)_k} \frac{z^k}{k!}. \quad (63)$$

Here, $(a)_k$ is a Pochhammer symbol. By substituting Eq. (54) into Eq. (61), we obtain the particular solution:

$$\bar{T}_p(x_0) = \frac{1}{\Gamma(2\varepsilon)\Gamma(1-\varepsilon)} G_{3,3}^{2,3} \left(x_0 \left| \begin{matrix} 1, 1, 2(1-\varepsilon) \\ 1, 1-\varepsilon, 0 \end{matrix} \right. \right), \quad (64)$$

where, $\Gamma(\varepsilon)$ denotes the complete gamma function, and $G_{p,q}^{m,n} \left(z \left| \begin{matrix} a_1, a_2, \dots, a_p \\ b_1, b_2, \dots, b_q \end{matrix} \right. \right)$ is the Meijer G -function.

The general solution of ODE (46) is given by

$$\bar{T}_g = \bar{T}_c + \bar{T}_p, \quad (65)$$

which is the sum of the complementary solution, Eq. (62), and the particular solution, Eq. (62), and can be expressed as:

$$\bar{T}_g(x_0) = c_2 - c_1 \beta_{1-x_0}(1-\varepsilon, 1-\varepsilon) + \frac{1}{\Gamma(2\varepsilon)\Gamma(1-\varepsilon)} G_{3,3}^{2,3} \left(x_0 \left| \begin{matrix} 1, 1, 2(1-\varepsilon) \\ 1, 1-\varepsilon, 0 \end{matrix} \right. \right). \quad (66)$$

Using the boundary conditions, we determine the normalization constants c_1 and c_2 . We then derive an expression for the MFPT, \bar{T}_{LH} , which explicitly incorporates the effects of the absorbing boundaries. Recall that the noisy voter model is defined on the interval $x \in [0, 1]$. We begin by setting absorbing boundaries at points L and H , with $0 \leq L < H \leq 1$. As before, L represents the lower boundary and H the upper boundary. The absorbing boundary conditions require that

the general solution of the ODE (46) satisfies the following constraints:

$$\bar{T}_g(L) = 0, \quad (67)$$

and

$$\bar{T}_g(H) = 0. \quad (68)$$

Combining Eqs. (66), (67), and (68), we find that the MFPT with absorbing boundaries at both ends is given by

$$\bar{T}_{LH} = \frac{\bar{T}_p(H) \beta_{1-L} - \bar{T}_p(L) \beta_{1-H}}{\beta_{1-H} - \beta_{1-L}} + \frac{\bar{T}_p(L) - \bar{T}_p(H)}{\beta_{1-H} - \beta_{1-L}} \beta_{1-x_0} + \bar{T}_p(x_0). \quad (69)$$

In the above $\beta_z = \beta_z(1 - \varepsilon, 1 - \varepsilon)$ is the incomplete beta function (the frequently repeated arguments have been omitted for brevity), and $\bar{T}_p(z)$ is a particular solution of Eq. (46), which is given by is given by Eq. (64).

If we place a reflective boundary at L instead of using Eq (67), the general solution $\bar{T}_g(x_0)$ must satisfy:

$$\left. \frac{d}{dx_0} \bar{T}_g \right|_{x_0=L} = 0. \quad (70)$$

By substituting Eq. (66) into Eq. (70) and differentiating with respect to x_0 , we determine the first normalization constant:

$$c_1(L) = \beta_L(\varepsilon, \varepsilon) - \frac{\Gamma(\varepsilon) \Gamma(\varepsilon)}{\Gamma(2\varepsilon)}. \quad (71)$$

Next, inserting Eqs. (66) into Eq. (68) gives the second normalization constant:

$$c_2 = c_1(L) \beta_{1-H}(1 - \varepsilon, 1 - \varepsilon) - \bar{T}_p(H). \quad (72)$$

Inserting Eqs. (71) and (72) into Eq. (66), we obtain the MFPT for the scenario with a reflective boundary at boundary at L and absorbing boundary at H :

$$\bar{T}_r = \left(\frac{\Gamma(\varepsilon) \Gamma(\varepsilon)}{\Gamma(2\varepsilon)} - \beta_L(\varepsilon, \varepsilon) \right) (\beta_{1-x_0} - \beta_{1-H}) + \bar{T}_p(x_0) - \bar{T}_p(H). \quad (73)$$

For simplicity, we define $\bar{T}_r = \bar{T}_{L_r H_a}(x_0)$. From this point on, \bar{T}_r will always denote the MFPT with a reflective boundary at the lower limit L and an absorbing boundary at the upper limit H .

The expressions for MFPT given in Eqs. (69) and (73) are rather complex; however, we can derive simpler approximations for large values of ε . When the rate ε is large, the influence of x_0 and L in Eq (73) becomes negligible, allowing the MFPT to be approximated by:

$$\bar{T}_r = -\frac{\Gamma(\varepsilon) \Gamma(\varepsilon)}{\Gamma(2\varepsilon)} \beta_{1-H}(1 - \varepsilon, 1 - \varepsilon). \quad (74)$$

To simplify Eq (74), we use the following identity:

$$\frac{\Gamma(\varepsilon) \Gamma(\varepsilon)}{\Gamma(2\varepsilon)} = \beta(\varepsilon, \varepsilon), \quad (75)$$

where $\beta(a, b)$ is the Euler beta function, defined by the integral

$$\beta(a, b) = \int_0^1 r^{a-1} (1-r)^{b-1} dr. \quad (76)$$

By applying the series expansion for large ε , the Euler beta function can be approximated as

$$\beta(\varepsilon, \varepsilon) = \frac{2\sqrt{\pi}}{2^{2\varepsilon} \sqrt{\varepsilon}} + \dots, \quad (77)$$

and the incomplete beta function as

$$\beta_{1-H}(1 - \varepsilon, 1 - \varepsilon) \simeq -\frac{1}{\varepsilon} \frac{H}{(1-H)^{-\varepsilon} H^{-\varepsilon}}. \quad (78)$$

Substituting Eqs. (77) and (78) into Eq. (74), we obtain:

$$\bar{T}_r \simeq \frac{2\sqrt{\pi}}{2^{2\varepsilon} \varepsilon^{3/2}} \cdot \frac{H}{(1-H)^\varepsilon H^\varepsilon} = \frac{2\sqrt{\pi} H}{\varepsilon^{3/2}} e^{-\varepsilon \ln \left[\frac{1}{4H(1-H)} \right]}. \quad (79)$$

From Eq. (79), it follows that the MFPT with a reflective boundary at L grows exponentially as the transition rate ε increases, i.e. $\bar{T}_r \sim e^\varepsilon$. A similar exponential growth can be demonstrated for the case with two absorbing boundaries, where $\bar{T}_{LH} \sim e^\varepsilon$.

Here, we derived an approximation for the MFPT with a reflective boundary at L and an absorbing boundary at H . This problem is equivalent to the case where the reflection is at H and absorption at L . The results for this case could be obtained simply by swapping $L \rightarrow H$ and $H \rightarrow L$.

Mean first passage time for integer ε values

In the context of the noisy voter model, ε represents the independent transition rate and must be a non-negative real number. Thus, the range of possible ε values includes natural numbers (non-negative integers). The general solutions for the noisy voter model we have obtained in this work involve quite a few instances of the incomplete beta function $\beta_z(a, b)$, which is indeterminate when a or b is a negative integer. This is an issue, as we often have that $a = b = 1 - \varepsilon$. Hence, for a certain integer ε values, the general solution we have obtained would be indeterminate. However, these cases can be treated independently by finding the solution directly from the ODE (46).

Let us return to the general form of the complementary solution (see Eq. (52))

$$\bar{T}_c = c_2 + c_1 \int \frac{1}{x_0^n (1-x)^n} dx_0. \quad (80)$$

Here, we set $\varepsilon = n$. When n is a natural number, integrating the function

$$I(x) = \frac{1}{x^n (1-x)^n}, \quad (81)$$

requires breaking it down into partial fractions. To begin, we express the decomposition as:

$$I(x) = \frac{1}{x^n (1-x)^n} = \sum_{i=1}^n \left[\frac{A_i(n)}{x^i} + \frac{B_i(n)}{(1-x)^i} \right], \quad (82)$$

where A_i and B_i are constants to be determined. These coefficients are typically obtained by multiplying both sides of the equation by $x^n (1-x)^n$ and matching coefficients of like powers. Alternatively, one can evaluate suitable derivatives at $x = 0$ and $x = 1$. In practice, solving for the values of $A_i(n)$ and $B_i(n)$ becomes increasingly complex as n grows, because it involves solving a coupled system of linear equations that scales with n . No simple closed-form expressions exist for $A_i(n)$ and $B_i(n)$, and the values vary across n ; for example, $A_1(1) \neq A_1(2) \neq \dots \neq A_1(n)$. Therefore, the coefficients must be computed case by case for each specific integer value of n .

By substituting Eqs. (80) and (61) (in place of Eqs. (54) and (64)) into Eq. (69), we obtain an expression for the MFPT that is valid for integer values of the transition rate.

For the scenario where both L and H are absorbing boundaries, the corresponding MFPT is given by:

$$\bar{T}_{LH} = \frac{M_n(H) Q_n(L) - M_n(L) Q_n(H)}{Q_n(H) - Q_n(L)} + \frac{M_n(L) - M_n(H)}{Q_n(H) - Q_n(L)} Q_n(x_0) + M_n(x_0), \quad (83)$$

where the auxiliary functions are defined as:

$$M_n(z) = \int^z (r(1-r))^{n-1} \int^r \frac{1}{q^n (1-q)^n} dq dr - \int^z \frac{1}{r^n (1-r)^n} dr \int^r r^{n-1} (1-r)^{n-1} dr, \quad (84)$$

and

$$Q_n(z) = \int^z \frac{1}{r^n (1-r)^n} dr. \quad (85)$$

The MFPT for the case with a reflective boundary at L and an absorbing boundary at H is given by:

$$\bar{T}_r = (\beta(n, n) - Q_n(L)) (Q_n(x_0) - Q_n(H)) + M_n(x_0) - M_n(H), \quad \text{with } n \geq 1, \quad (86)$$

the functions $M_n(z)$ and $Q_n(z)$ are the same as in \bar{T}_{LH} , Eq. (83).

C Special cases

The general formulas for the MFPT, given in Eqs. (69) and (73), may at first seem difficult to evaluate due to the presence of special functions. However, for certain values of the transition rate ε , these expressions simplify significantly. In particular, when $\varepsilon = \frac{n}{2}$ with $n \in \mathbb{N}$, the MFPT can be written in terms of elementary functions—specifically, trigonometric and logarithmic functions, along with polynomials. For illustration, we present the special cases $\varepsilon \in \{0, \frac{1}{2}, 1, \frac{3}{2}\}$. With straightforward but careful algebra, similar formulas can be derived for larger values of n .

Detailed derivation for the $\varepsilon = 0$ case

In the limiting case $\varepsilon = 0$, the MFPT could be obtained by substituting this value into Eqs. (83) and (86). While the general-case derivation of the MFPT is quite involved—as detailed in A—here we provide a step-by-step derivation for the simplest case to aid readers interested in understanding the calculation. Specifically, when individualistic behavior is absent (i.e., $\varepsilon = 0$), the ODE (46) reduces to:

$$\frac{d^2}{dx_0^2} \bar{T}(x_0 | \varepsilon = 0) = -\frac{1}{x_0 (1-x_0)}. \quad (87)$$

The ODE (87) can be solved by direct integration, and the solution is

$$\bar{T}(x_0|\varepsilon=0) = c_1 + c_2 x_0 + (x_0 - 1) \ln(1 - x_0) + x_0 \ln x_0. \quad (88)$$

The absorbing boundary conditions require that the general solution of the ODE (88) satisfies the following constraints:

$$\bar{T}(L|\varepsilon=0) = 0, \quad (89)$$

and

$$\bar{T}(H|\varepsilon=0) = 0. \quad (90)$$

The normalization constants c_1 and c_2 can be determined using the boundary conditions introduced above. Substituting Eq. (88) into Eqs. (89) and (90) yield the following system of equations:

$$\begin{cases} c_1 + c_2 L + (L - 1) \ln(1 - L) + L \ln(L) = 0, \\ c_1 + c_2 H + (H - 1) \ln(1 - H) + H \ln(H) = 0. \end{cases} \quad (91)$$

By solving the system of equations above, we obtain the normalization constants:

$$c_1 = \frac{Lf(H) - Hf(L)}{H - L}, \quad \text{and} \quad c_2 = \frac{f(L) - f(H)}{H - L}. \quad (92)$$

Here, we introduce a placeholder function

$$f(z) = (z - 1) \ln(1 - z) - z \ln(z), \quad (93)$$

which allows us to greatly simplify the expressions for c_1 and c_2 expressions above. By substituting Eq. (92) into Eq. (88), we obtain the MFPT for the case with two absorbing boundaries:

$$\bar{T}_{LH}(x_0|\varepsilon=0) = \frac{Lf(L) - Hf(H)}{H - L} + \frac{f(L) - f(H)}{H - L} x_0 + f(x_0). \quad (94)$$

Let us set a reflective boundary at $L > 0$, since from the Fokker–Planck equation, Eq. (7), it is evident that the diffusion coefficient becomes zero at the end points of the interval $[0, 1]$. In this special case, there is no drift, so even if a reflective boundary is placed at the edge of the interval, there is no noise or drift to alter the value of x . As a result, reflective boundaries at the endpoints effectively behave as absorbing boundaries.

Therefore, to properly study the effect of a reflective boundary on the MFPT, we must ensure that the reflective boundary is placed strictly within the interval—that is, $L > 0$. If we assume a reflective boundary at point L , then instead of imposing $\bar{T}(L) = 0$, the condition from Eq. (92) becomes:

$$\left. \frac{d}{dx_0} \bar{T}(x_0|\varepsilon=0) \right|_{x_0=L} = 0. \quad (95)$$

By substituting Eq. (88) into Eq. (95), we obtain the normalization constant c_2 :

$$c_2 = \ln(L) - \ln(1 - L), \quad (96)$$

Then, by substituting Eq. (96) into the second equation (concerning boundary H) from Eq. (91), we find the other constant:

$$c_1 = H(\ln L - \ln(1 - L)) - f(H). \quad (97)$$

Here $f(z)$ is the same function as in the previous case (see Eq. (93)). By substituting Eqs. (96) and (97) into Eq. (88), we obtain MFPT for the case of reflective boundary at L

$$\bar{T}_r(x_0|\varepsilon=0) = (H - x_0)g(L) - f(H) + f(x_0). \quad (98)$$

Here, we have introduced a new placeholder function, which is defined as

$$g(z) = \ln(1 - z) - \ln(z) = 2 \arctan(1 - 2z). \quad (99)$$

Detailed derivation for the $\varepsilon = \frac{1}{2}$ case

This case is particularly intriguing because it can be derived in two distinct ways: either through our proposed approach or by applying a nonlinear transformation to the Fokker–Planck equation, effectively reducing it to a diffusion equation. We examine both methods in more detail below.

The nonlinear transformation is especially useful for analyzing the symmetry of the MFPT. However, for other values of ε , it introduces a nonlinear drift term, leaving the transformed Fokker–Planck equation just as complex as the original. Still, alternative transformations may exist that simplify the voter model by mapping it onto well-known stochastic processes—similar to techniques used in certain birth-death models [92]. This strategy has been successfully applied to the scaled voter model to approximate the FPTD [93].

In this case, we can use the relationship between the incomplete beta function $\beta_{1-z}(a, b)$ inverse trigonometric functions:

$$\beta_{1-z}(1-\varepsilon, 1-\varepsilon) \Big|_{\varepsilon=1/2} = \beta_{1-z}(1/2, 1/2) = 2 \arcsin(\sqrt{1-z}). \quad (100)$$

The Meijer G -function can also be expressed in terms of inverse trigonometric functions:

$$G_{3,3}^{2,3} \left(z \left| \begin{matrix} 1, 1, 1 \\ 1, 1/2, 0 \end{matrix} \right. \right) = \frac{\sqrt{\pi}}{2} \left(\pi^2 + (2 \operatorname{arccosh}(\sqrt{z}))^2 \right). \quad (101)$$

By substituting Eq. (101) into Eq. (64), we obtain the corresponding particular solution.

$$\bar{T}_p \left(z | \varepsilon = \frac{1}{2} \right) = \frac{1}{2} \left(\pi^2 + (2 \operatorname{arccosh}(\sqrt{z}))^2 \right) \quad (102)$$

Here we used the identity $\Gamma(1) \Gamma(\frac{1}{2}) = \sqrt{\pi}$.

By inserting Eqs. (100) and (102) back into Eq. (69), and applying properties of inverse trigonometric and inverse hyperbolic functions, we obtain the MFPT for absorbing boundaries:

$$\bar{T}_{LH} \left(x_0 | \varepsilon = \frac{1}{2} \right) = \frac{1}{2} \left(\arcsin(2x_0 - 1) - \arcsin(2L_x - 1) \right) \left(\arcsin(2H_x - 1) - \arcsin(2x_0 - 1) \right). \quad (103)$$

In the case of a reflective boundary at L , the formula for the MFPT includes a special function—the Euler beta function. One important identity to keep in mind is

$$\beta \left(\frac{1}{2}, \frac{1}{2} \right) = \pi. \quad (104)$$

To compute the MFPT, we substitute Eqs. (100), (102) and (104) into Eq. (73). Then, by applying properties of inverse hyperbolic functions, we arrive at the final expression for the MFPT under this boundary condition:

$$\begin{aligned} \bar{T}_r \left(x_0 | \varepsilon = \frac{1}{2} \right) &= \frac{1}{2} \cdot \left(\arcsin(2H - 1) - \arcsin(2x_0 - 1) \right) \\ &\cdot \left(\arcsin(2H - 1) - 2 \arcsin(2L - 1) + \arcsin(2x_0 - 1) \right). \end{aligned} \quad (105)$$

An alternative approach to deriving the MFPT involves applying a variable transformation to the Fokker–Planck equation or its corresponding SDE. In the special case where $\varepsilon = \frac{1}{2}$, we can use a nonlinear transformation of the form $y = \arcsin(2x - 1)$. By first applying this change of variables, the original Fokker–Planck equation (7) transforms into a new equation expressed in terms of the variable y :

$$\frac{\partial P(y, t | y_0, 0)}{\partial t} = \frac{\partial P(y, t | y_0, 0)}{\partial y^2}, \quad (106)$$

and the corresponding time-backward equation has identical form

$$\frac{\partial P(y, t | y_0, 0)}{\partial t} = \frac{\partial P(y, t | y_0, 0)}{\partial y_0^2}. \quad (107)$$

By comparing the equation above with the time-backward Fokker–Planck equation, Eq. (40), and using the previously established relation given in Fokker–Planck equation, Eq. (45), we arrive at the following ODE for the MFPT:

$$\frac{d^2}{dy_0^2} \bar{T}(y_0) = -1. \quad (108)$$

The ODE above can be solved by simple integration

$$\bar{T}(y_0) = c_1 + c_2 y_0 - \frac{y_0^2}{2} \quad (109)$$

The constants c_1 and c_2 can be determined by applying the absorbing boundary conditions at the points L_y and H_y . These boundaries are introduced by enforcing that the MFPT satisfies $\bar{T}(L_y) = 0$ and $\bar{T}(H_y) = 0$. From these conditions, it follows that:

$$\begin{cases} \bar{T}(L_y) = c_1 + c_2 L_y - \frac{L_y^2}{2} = 0, \\ \bar{T}(H_y) = c_1 + c_2 H_y - \frac{H_y^2}{2} = 0. \end{cases} \quad (110)$$

From the system of equations above, we find that:

$$c_1 = \frac{1}{2} H_y L_y, \quad \text{and} \quad c_2 = \frac{1}{2} (H_y + L_y). \quad (111)$$

Substituting the values of c_1 and c_2 into Eq. (109), we obtain the MFPT in the y -space corresponding to the boundaries

L_y and H_y :

$$\bar{T}_{LH}(y_0) = \frac{1}{2} (y_0 - L_y) (H_y - y_0). \quad (112)$$

Recalling the relationship between the variables y and x , given by:

$$y = \arcsin(2x - 1), \quad (113)$$

and substituting it into Eq. (112), we obtain the MFPT in terms of x :

$$\bar{T}_{LH}(x_0) = \frac{1}{2} (\arcsin(2x_0 - 1) - \arcsin(2L - 1)) (\arcsin(2H - 1) - \arcsin(2x_0 - 1)) \quad (114)$$

We now turn to the symmetry properties of the MFPT in the presence of absorbing boundaries. Our goal is to determine the location and nature of the function's maximum, and to identify the conditions under which the MFPT is symmetric about this point.

The MFPT in y -space, given in Eq. (112), is a quadratic function of the initial position y_0 , and therefore describes a parabola. Since parabolic functions are symmetric about their vertex, we first identify the vertex location:

$$y_{0,\max} = \frac{H_y + L_y}{2}. \quad (115)$$

To obtain the corresponding value of x_0 , we invert the original transformation:

$$x_0 = \frac{1}{2} (1 + \sin(y_0)). \quad (116)$$

Substituting the vertex location from Eq. (115) into Eq. (116), we find that the maximum of the MFPT occurs at:

$$x_{0,\max} = \frac{1}{2} \left(1 + \sin\left(\frac{H_y + L_y}{2}\right) \right). \quad (117)$$

We now examine whether the function is symmetric about this point. That is, whether

$$\bar{T}_{LH}\left(x_0|\varepsilon = \frac{1}{2}\right) = \bar{T}_{LH}\left(1 - x_0|\varepsilon = \frac{1}{2}\right) \quad (118)$$

holds. Since the transformation $x_0 = \frac{1}{2} [1 + \sin(y_0)]$ is both monotonic and smooth, any symmetry in y_0 directly translates to symmetry in x_0 . In particular, symmetry about the vertex occurs when the quadratic is centered at $y_0 = 0$, which leads to the condition:

$$H_y = -L_y \quad \Rightarrow \quad \arcsin(2H - 1) = -\arcsin(2L - 1). \quad (119)$$

Applying the identity $\arcsin(-z) = -\arcsin(z)$, we obtain the symmetry condition:

$$2H - 1 = -(2L - 1), \quad (120)$$

which simplifies to:

$$H = 1 - L. \quad (121)$$

This means the interval $[L, H]$ is centered at $\frac{1}{2}$. Any point x_0 within this interval has a mirror point $1 - x_0$ that is equally distant from the midpoint. Because the boundaries are placed symmetrically, the behavior of the stochastic process is also symmetric, and so is the MFPT. This condition can be expressed more explicitly by setting:

$$L = \frac{1}{2} - d, \quad H = \frac{1}{2} + d, \quad \text{with } 0 < d \leq \frac{1}{2}. \quad (122)$$

Therefore, we conclude that the same symmetry condition holds for the case $\varepsilon = \frac{1}{2}$ as for the case $\varepsilon = 0$.

In the case of a reflecting boundary at $y_0 = L_y$ and an absorbing boundary at $y_0 = H_y$, the constants c_1 and c_2 can be determined by applying the boundary conditions:

$$\frac{d}{dy_0} \bar{T}(L_y) = 0, \quad \text{if } \bar{T}(H_y) = 0. \quad (123)$$

From the absorbing boundary condition, we have:

$$\bar{T}(H_y) = c_1 + c_2 H_y - \frac{H_y^2}{2} = 0. \quad (124)$$

This allows us to obtain the expression for the first constant:

$$c_1 = \frac{1}{2} H_y (H_y - 2c_2) \quad (125)$$

Substituting c_1 back into Eq. (109), we obtain:

$$\bar{T}_H(y_0) = \frac{1}{2} H_y (H_y - 2c_2) + c_2 y_0 - \frac{y_0^2}{2}. \quad (126)$$

Applying the reflecting boundary condition:

$$\left. \frac{d}{dy_0} \bar{T}_H \right|_{y_0=L_y} = c_2 - L_y = 0, \quad \Rightarrow \quad c_2 = L_y. \quad (127)$$

Substituting c_2 back into Eq. (109), we arrive at the final expression:

$$\bar{T}_r(y_0) = \frac{1}{2} (H_y - y_0) (H_y - 2L_y + y_0). \quad (128)$$

Recalling the relationship between the variables y and x , given in Eq. (113), we obtain the MFPT in x -space

$$\begin{aligned} \bar{T}_r(x_0) &= \frac{1}{2} \cdot (\arcsin(2H - 1) - \arcsin(2x_0 - 1)) \\ &\quad \cdot (\arcsin(2H - 1) - 2\arcsin(2L - 1) + \arcsin(2x_0 - 1)). \end{aligned} \quad (129)$$

The obtained MFPT expressions, Eqs. (128) and (129), are identical to the expressions obtained from the general solution, Eqs. (103) and (105).

Detailed derivation for the $\varepsilon = 1$ case

Let us derive the MFPT for the case where the transition rate parameter is set to $\varepsilon = 1$. For the case with two absorbing boundaries, we demonstrate that the boundary values proposed in previous sections—namely $L = \frac{1}{2} - d$ and $H = \frac{1}{2} + d$ —result in an MFPT that remains symmetric concerning the midpoint of the interval $[L, H]$. We also consider the case when at L we have reflective boundary instead.

If we set $\varepsilon = 1$, the integral in in Eq. (80) involves the kernel $\nu(x_0)$. Partial fraction decomposition of the said kernel, according to to Eq. (82), is given by

$$\frac{1}{x_0(1-x_0)} = \frac{1}{x_0} + \frac{1}{x_0(1-x_0)}. \quad (130)$$

Thus the complementary solution is

$$\bar{T}_c = c_2 - c_1 (\ln(x_0) - \ln(1-x_0)). \quad (131)$$

Using the complementary solution \bar{T}_c and applying the method of variation of parameters, we obtain the particular solution

$$\bar{T}_p = \ln(1-x_0) \quad (132)$$

The general solution is given by $\bar{T}_g = \bar{T}_c + \bar{T}_p$, which is the sum of the complementary solution, Eq. (131), and the particular solution, Eq. (132), and can be expressed as:

$$\bar{T}_g = c_2 - c_1 \ln\left(\frac{x_0}{1-x_0}\right) + \ln(1-x_0). \quad (133)$$

The presence of absorbing boundaries requires that $\bar{T}_g(L) = 0$ and $\bar{T}_g(H) = 0$. Therefore, the MFPT for two absorbing boundaries is given by:

$$\bar{T}_{LH}(x_0|\varepsilon=1) = \frac{\ln(H) \ln\left(\frac{1-L}{1-x_0}\right) + \ln(L) \ln\left(\frac{1-x_0}{1-H}\right) + \ln(x_0) \ln\left(\frac{1-H}{1-L}\right)}{\ln\left(\frac{H}{1-H}\right) + \ln\left(\frac{L}{1-L}\right)}. \quad (134)$$

We can rewrite the MFPT in a more compact form:

$$\bar{T}_{LH}(x_0|\varepsilon=1) = \frac{1}{c_{LH}} (K(H, L, x_0) + K(L, x_0, H) + K(x_0, H, L)) \quad (135)$$

Here, we define $K(a, b, c) = \ln(a) \ln\left(\frac{1-b}{1-c}\right)$, and introduce the normalization factor as follows:

$$c_{LH} = \ln\left(\frac{H}{1-H}\right) + \ln\left(\frac{L}{1-L}\right) = 2(\arctan(1-2H) - \arctan(1-2L)). \quad (136)$$

The formula for the MFPT, given by Eq. (134), can be significantly simplified if we choose absorbing boundaries that are symmetric concerning the the midpoint $\frac{1}{2}$ of the domain. This symmetry means that the MFPT is invariant under the transformation $x_0 \rightarrow 1 - x_0$ when $\varepsilon = 1$, i.e.,

$$\bar{T}_{LH}(x_0|\varepsilon=1) = \bar{T}_{LH}(1-x_0|\varepsilon=1). \quad (137)$$

To make the notation more compact, we introduce the following logarithmic variables:

$$\begin{aligned} A &= \ln(H), & B &= \ln(L), & C &= \ln(x_0), \\ D &= \ln(1-H), & E &= \ln(1-L), & F &= \ln(1-x_0). \end{aligned} \quad (138)$$

With these definitions, Eq. (134) becomes

$$\bar{T}_{LH}(x_0|\varepsilon=1) = A(E-F) + B(F-D) + C(D-E) \quad (139)$$

The symmetry condition can be enforced by requiring

$$\bar{T}_{LH}(x_0|\varepsilon=1) - \bar{T}_{LH}(1-x_0|\varepsilon=1) = 0, \quad (140)$$

Substituting the Eq. (134) into Eq. (140) and simplifying leads to:

$$(A - B + D - E)(C - F) = 0, \quad (141)$$

This equation admits two possible solutions:

$$C - F = 0 \quad \Rightarrow \quad x = \frac{1}{2}, \quad (142)$$

and

$$A - B + D - E = 0 \quad \Rightarrow \quad \frac{H(1-H)}{L(1-L)} = 1 \quad \Rightarrow \quad H = 1 - L. \quad (143)$$

To express the symmetric-boundary case more explicitly, let us introduce a small positive parameter $d \leq \frac{1}{2}$ that measures the distance of the boundaries from the midpoint. Let us set that $L = \frac{1}{2} - d$. Thus, form $H = 1 - L$. follows the absorbing boundaries must satisfy:

$$L = \frac{1}{2} - d, \quad \Rightarrow \quad H = \frac{1}{2} + d. \quad (144)$$

By inserting this parametrization into Eq. (134), we obtain a simplified closed-form expression for the MFPT under symmetric absorbing boundaries.

$$\begin{aligned} \bar{T}_{\frac{1}{2}-d, \frac{1}{2}+d}(x_0|\varepsilon=1) &= \frac{1}{c_{\frac{1}{2}-d, \frac{1}{2}+d}} \left[\ln\left(\frac{1}{2} + d\right) \left\{ \ln\left(\frac{1}{2} + d\right) - \ln(x_0(1-x_0)) \right\} \right. \\ &\quad \left. + \ln\left(\frac{1}{2} - d\right) \left\{ \ln(x_0(1-x_0)) + \ln\left(\frac{1}{2} - d\right) \right\} \right]. \end{aligned} \quad (145)$$

The MFPT with a reflective boundary at L , as given in Eq. (135), can also be derived from Eq. (86) by setting $n = 2$:

$$\bar{T}_r = -(1-L)\ln(1-H) - L\ln(H) + L(\ln(x_0) - \ln(1-x_0)) + \ln(1-x_0). \quad (146)$$

Detailed derivation for the $\varepsilon = \frac{3}{2}$ case

In this section, we derive the MFPT for a system with a transition rate parameter set to $\varepsilon = \frac{3}{2}$. We consider two configurations: one with absorbing boundaries and another with a reflective boundary at the point L . For the case with two absorbing boundaries, we demonstrate that the boundary values proposed in previous sections—namely $L = \frac{1}{2} - d$ and $H = \frac{1}{2} + d$ —result in an MFPT that remains symmetric concerning the midpoint of the interval $[L, H]$. In this case, we can use the relationship between the incomplete beta function $\beta_{1-z}(a, b)$ inverse trigonometric functions:

$$\beta_{1-z}\left(-\frac{1}{2}, -\frac{1}{2}\right) = \frac{2(1-2z)}{\sqrt{z(1-z)}}. \quad (147)$$

The Meijer G -function can also be expressed in terms of inverse trigonometric functions:

$$G_{3,3}^{2,3}\left(z \left| \begin{matrix} -1, 1, 1 \\ -\frac{1}{2}, 1, 0 \end{matrix} \right. \right) = 2\sqrt{\pi} \left(1 + \frac{(1-2z)\arccos(\sqrt{z})}{\sqrt{z(1-z)}} \right). \quad (148)$$

By substituting Eq. (148) into Eq. (64), we obtain the corresponding particular solution:

$$\bar{T}_p\left(x_0|\varepsilon = \frac{3}{2}\right) = -\frac{1}{4\sqrt{\pi}} G_{3,3}^{2,3}\left(z \left| \begin{matrix} -1, 1, 1 \\ -\frac{1}{2}, 1, 0 \end{matrix} \right. \right) = \frac{1}{2} \left(\frac{(2x_0-1)\arccos(\sqrt{x_0})}{\sqrt{x_0(1-x_0)}} - 1 \right), \quad (149)$$

Here we used the gamma $\Gamma(z)$ function property:

$$\frac{1}{\Gamma(3)\Gamma(-\frac{1}{2})} = -\frac{1}{4\sqrt{\pi}} \quad (150)$$

By inserting Eqs. (147), (149) back into Eq. (69), and applying properties of inverse trigonometric and inverse hyperbolic functions, we obtain the MFPT for absorbing boundaries:

$$\begin{aligned} \bar{T}_{LH} \left(x_0 | \varepsilon = \frac{3}{2} \right) &= \frac{1}{2 \left(\frac{1-2H}{\sqrt{(1-H)H}} - \frac{1-2L}{\sqrt{(1-L)L}} \right)} \left\{ \frac{1-2H}{\sqrt{(1-H)H}} \left(1 + \frac{(1-2L) \arccos(\sqrt{L})}{\sqrt{(1-L)L}} \right) \right. \\ &\quad - \frac{1-2L}{\sqrt{(1-L)L}} \left(1 + \frac{(1-2H) \arccos(\sqrt{H})}{\sqrt{(1-H)H}} \right) \\ &\quad + \frac{1-2x_0}{\sqrt{(1-x_0)x_0}} \left(\frac{(1-2H) \arccos(\sqrt{H})}{\sqrt{(1-H)H}} - \frac{(1-2L) \arccos(\sqrt{L})}{\sqrt{(1-L)L}} \right) \Big\} \\ &\quad - \frac{1}{2} \left(1 + \frac{(1-2x_0) \arccos(\sqrt{x_0})}{\sqrt{(1-x_0)x_0}} \right). \end{aligned} \quad (151)$$

In the case of a reflective boundary at L , the formula for the MFPT includes a special function—the Euler beta function. One important identity to keep in mind is

$$\beta \left(\frac{1}{2}, \frac{1}{2} \right) = \frac{\pi}{8}. \quad (152)$$

To compute the MFPT, we substitute Eqs. (152), (147) and (149) into Eq. (73). Then, by applying properties of inverse hyperbolic functions, we arrive at the final expression for the MFPT under this boundary condition:

$$\begin{aligned} \bar{T}_r \left(x_0 | \varepsilon = \frac{3}{2} \right) &= \frac{1}{2} \left(1 + \frac{(1-2H) \arccos(\sqrt{H})}{\sqrt{(1-H)H}} \right) \\ &\quad + \frac{1}{8} \left(\frac{2(1-2x_0)}{\sqrt{(1-x_0)x_0}} - \frac{2(1-2H)}{\sqrt{(1-H)H}} \right) \left(\frac{2(1-2L)(1-L)L}{\sqrt{(1-L)L}} + 2 \arccos(\sqrt{L}) \right) \\ &\quad - \frac{1}{2} \left(1 + \frac{(1-2x_0) \arccos(\sqrt{x_0})}{\sqrt{(1-x_0)x_0}} \right). \end{aligned} \quad (153)$$

However, the expressions for \bar{T}_{LH} and \bar{T}_r retain the same functional form as in Eq. (69). They remain quite complex, and little simplification is possible unless additional constraints are introduced. Let us assume that the boundaries are placed symmetrically around the midpoint

$$L = \frac{1}{2} - d, \quad H = \frac{1}{2} + d, \quad \text{with } 0 < d \leq \frac{1}{2}. \quad (154)$$

By making this assumption, we arrive at a useful relationship:

$$\bar{T}_p \left(\frac{1}{2} + d | \varepsilon = \frac{3}{2} \right) - \bar{T}_p \left(\frac{1}{2} - d | \varepsilon = \frac{3}{2} \right) = \frac{\pi d}{\sqrt{1-4d}}, \quad (155)$$

To obtain the relation above, we applied the identity:

$$\arccos \left(\sqrt{\frac{\pi}{2} + d} \right) + \arccos \left(\sqrt{\frac{\pi}{2} - d} \right) = \frac{\pi}{2}. \quad (156)$$

By substituting Eqs. (154) and (155) into Eq. (69), we derive the MFPT

$$\begin{aligned} \bar{T}_{\frac{1}{2}-d, \frac{1}{2}+d} \left(x_0 | \varepsilon = \frac{3}{2} \right) &= \frac{d}{\sqrt{1-4d^2}} \left(\arccos \left(\sqrt{\frac{1}{2} - d} \right) - \arccos \left(\sqrt{\frac{1}{2} + d} \right) \right) \\ &\quad + \frac{1-2x_0}{2\sqrt{(1-x_0)x_0}} \left(\frac{\pi}{4} - \arccos(\sqrt{x_0}) \right). \end{aligned} \quad (157)$$

The first term ensures that $\bar{T}_{\frac{1}{2}-d, \frac{1}{2}+d} (x_0 | \varepsilon = \frac{3}{2})$ vanishes at the selected absorbing boundaries, while the second term corresponds to the mean consensus time, $\bar{T}_{01} (x_0 | \varepsilon = \frac{3}{2})$. Comparing this expression to the earlier Eq. (151), we see that all terms responsible for the asymmetry have disappeared. In principle, the same approach can be applied to any $\varepsilon = \frac{n}{2}$, with $n \in \mathbb{N}$, since the MFPT expressions involve trigonometric, logarithmic, and polynomial functions—all of which possess inherent symmetries.